DETERMINATION OF PROBABILITY OF INTERNAL EROSION IN
EARTHEN DAM SEEPAGE

A THESIS SUBMITTED TO
THE GRADUATE SCHOOL OF NATURAL AND APPLIED SCIENCES
OF
MIDDLE EAST TECHNICAL UNIVERSITY

BY

OĞULCAN YANAR

IN PARTIAL FULFILLMENT OF THE REQUIREMENTS
FOR
THE DEGREE OF MASTER OF SCIENCE
IN
CIVIL ENGINEERING

JANUARY 2024

Approval of the thesis:

DETERMINATION OF PROBABILITY OF INTERNAL EROSION IN EARTHEN DAM SEEPAGE

submitted by **OĞULCAN YANAR** in partial fulfillment of the requirements for the degree of **Master of Science** in **Civil Engineering, Middle East Technical University** by,

Prof. Dr. Halil Kalıpçılar
Dean, Graduate School of **Natural and Applied Sciences**   _____

Prof. Dr. Erdem Canbay
Head of the Department, **Civil Engineering Department**   _____

Assoc. Prof. Dr. Melih Çalamak
Supervisor, **Civil Engineering Department, METU**   _____

Examining Committee Members:

Prof. Dr. A. Melih Yanmaz
Civil Engineering Dept., METU   _____

Assoc. Prof. Dr. Melih Çalamak
Civil Engineering Dept., METU   _____

Assist. Prof. Dr. Cüneyt Baykal
Civil Engineering Dept., METU   _____

Assoc. Prof. Dr. Meriç Yılmaz
Civil Engineering Dept., Atılım University   _____

Assoc. Prof. Dr. Müsteyde Baduna Koçyiğit
Civil Engineering Dept., Gazi University   _____

Date: 26.01.2024

I hereby declare that all information in this document has been obtained and presented in accordance with academic rules and ethical conduct. I also declare that, as required by these rules and conduct, I have fully cited and referenced all material and results that are not original to this work.

Name Last name : Oğulcan Yanar

Signature :

iv

ABSTRACT

DETERMINATION OF PROBABILITY OF INTERNAL EROSION IN EARTHEN DAM SEEPAGE

Yanar, Oğulcan
Master of Science, Civil Engineering
Supervisor: Assoc. Prof. Dr. Melih Çalamak

January 2024, 62 pages

Piping, caused by internal erosion, is one of the main failure modes of earthen dams. In this study, a probabilistic modeling framework was proposed to determine the reliability of an earthen dam against internal erosion. The uncertainties associated with the mechanisms governing the soil internal erosion were considered to assess the probability of internal erosion and piping failure. To this end, probabilistic seepage analyses were conducted using the finite element method to determine the maximum hydraulic gradient. Then, the critical hydraulic gradient was determined by taking the probabilistic nature of soil parameters into account. The Monte Carlo method was applied for the analyses. The histogram and the probability density function of the critical hydraulic gradient were produced for an existing earthen dam. Then, the probability of exceedance of the critical hydraulic gradient was computed to assess the reliability of the structure. The earthen dam was found to be highly susceptible to internal erosion according to the calculated exceedance probabilities. Model results were further investigated to comment on the probability of internal erosion and piping. Additionally, two alternative designs with seepage control measures were suggested and their performances were evaluated.

Keywords: Earthen dams, Internal Erosion, Piping, Finite-element Method, Monte Carlo Simulation, Risk Analysis

ÖZ

TOPRAK BARAJLARDAKİ SIZMADA İÇSEL EROZYON OLASILIĞININ BELİRLENMESİ

Yanar, Oğulcan
Yüksek Lisans, İnşaat Mühendisliği
Tez Yöneticisi: Doç. Dr. Melih Çalamak

Ocak 2024, 62 sayfa

İçsel erozyonun sebep olduğu borulanma, toprak dolgu barajların başlıca yıkılma sebeplerinden biridir. Bu çalışmada, bir dolgu barajın içsel erozyon güvenilirliğinin belirlenmesi için bir modelleme yöntemi önerilmiştir. İçsel erozyon ve borulanma göçmesi olasılığının belirlenmesi için içsel erozyonu yöneten mekanizmalarla ilgili belirsizlikler göz önünde bulundurulmuştur. Bu amaçla, sonlu elemanlar yöntemi kullanılarak olasılıksal sızma analizleri yapılmış ve maksimum hidrolik eğim belirlenmiştir. Daha sonra zemin parametrelerinin olasılıksal yapısı dikkate alınarak kritik hidrolik eğim belirlenmiştir. Olasılıksal analiz için Monte Carlo yöntemi uygulanmıştır. Kritik hidrolik eğimin histogramı ve olasılık yoğunluk fonksiyonu, mevcut bir dolgu baraj için üretilmiştir. Daha sonra yapının güvenilirliğini değerlendirmek için kritik hidrolik eğimin aşılma olasılığı hesaplanmıştır. Hesaplanan aşılma olasılığına göre, toprak barajın içsel erozyona karşı oldukça duyarlı olduğu tespit edilmiştir. Model sonuçları, içsel erozyon ve borulanma olasılığı ile ilgili yorum yapılması amacıyla, daha detaylı incelenmiştir. Ayrıca sızma kontrolü önlemlerine sahip iki alternatif tasarım önerilmiş ve performansları değerlendirilmiştir.

Anahtar Kelimeler: Dolgu barajlar, İçsel Erozyon, Borulanma, Sonlu Farklar Metodu, Monte Carlo Simülasyonu, Risk Analizi

To our great leader and teacher Mustafa Kemal ATATÜRK

ACKNOWLEDGMENTS

TABLE OF CONTENTS

LIST OF TABLES

LIST OF FIGURES

FIGURES

LIST OF ABBREVIATIONS

ABBREVIATIONS

CLR	Common Language Runtime
COV	Coefficient of Variation
FEM	Finite-element Method
FORM	First Order Reliability Method
FOSM	First Order Second Moment Method
GEV	Generalized Extreme Value
MCS	Monte Carlo Simulations
MVFOSM	Mean Value First Order Second Moment Method
PDF	Probability Density Function
PWP	Pore Water Pressure
RIC	Reliability Index Calculator
SWCC	Soil Water Characteristic Curve

LIST OF SYMBOLS

SYMBOLS

d	Downstream slope cover (m)
e_0	Initial void ratio
F_B	Freeboard (m)
g	Limit state function
G_S	Specific Gravity of soil
h	Water head (m)
h'	Reservoir water depth (m)
H_{crit}	The critical head (m)
i_{crit}	The critical hydraulic gradient
i_{max}	The maximum hydraulic gradient
K	Hydraulic conductivity (m/s)
K_r	Relative hydraulic conductivity
K_S	Saturated hydraulic conductivity (m/s)
K_x	Hydraulic conductivity in x-direction (m/s)
K_y	Hydraulic conductivity in y-direction (m/s)
K_z	Hydraulic conductivity in z-direction (m/s)
l	Drain length (m)
l_{max}	Maximum drain length (m)
l_{min}	Minimum drain length (m)
m	A fitting parameter of van Genuchten model

m'	Upstream face slope of the dam
n	A fitting parameter of van Genuchten model
n'	Downstream face slope of the dam
p	Pressure head (m)
R	Resistance
r	Box-Muller transformation variable
S	Demand
S_S	Specific Storage (m^{-1})
SF	Shape factor in Tao's model
T	Crest width of the dam (m)
t	Time (s)
u_1	Independent random variable 1
u_2	Independent random variable 2
x-Gradient	Hydraulic gradient in x-direction
y-Gradient	Hydraulic gradient in y-direction
xy-Gradient	Hydraulic gradient in xy-direction
α	A fitting parameter of van Genuchten model
β	Reliability index
γ'	Buoyant unit weight of soil (kN/m^3)
γ_w	Unit weight of water (kN/m^3)
μ	Mean
μ_K	Mean hydraulic conductivity (m/s)

μ_{lnK}	Mean of the natural logarithm of hydraulic conductivity
σ	Standard deviation
σ_K	Standard deviation of hydraulic conductivity (m/s)
σ_{lnK}	Standard deviation of the natural logarithm of hydraulic conductivity

CHAPTER 1

INTRODUCTION

1.1 General

Seepage in earthen dams is the percolation of water through the body and foundation and is always expected at certain levels. However, due to particular reasons, water flowing through the porous medium may carry away fine soil particles such as clay, silt, sand, and even gravel. The soil particles being removed by the water within the dam body or foundation is called internal erosion, and it is a major concern for earthen dams. If the internal erosion continues and progresses over time, it may create concentrated channels, also known as pipes, and results in a phenomenon called piping. Failures caused by internal erosion and piping are very rapid and catastrophic, especially for the downstream environment and settlements. Known as one of the largest dam failures in the United States, the Teton Dam failure in 1976 was caused by internal erosion that gradually developed into piping, leaving 14 people dead and millions of dollars of damage (Seed & Duncan, 1987). Another historical example of piping failure is the 1963 Baldwin Dam incident, which resulted in 5 deaths and millions of dollars in damages leading to changes in dam design and safety guidelines (ASDSO, 2023a). It is reported that 43% of historical dam failures were caused by piping (Foster et al., 2000). Most of the piping-related failed earthen dams do not have photographic evidence of the piping itself, rather they have photos after the incident. Figure 1.1 is a rare example of an earthen dam piping incident, although the location and date of the incident are not known.

Figure 1.1 An aerial photo from an earthen dam subject to excessive internal erosion. The location is not known (Belcher et al., 2016).

Internal erosion does not always result in piping. If the erosion rate is slightly low and the movement of fine soil particles is limited, there may not be enough of a concentrated channel so that a pipe can develop. Figure 1.2 shows various failure observations for an earthen dam. For example, the observation marked as "internal erosion" on the right side of the figure is not yet a concentrated channel and cannot be classified as piping. However, the observation labeled "seepage" on the left is an example of an internal erosion that has evolved into piping. Therefore, piping is always a result of internal erosion, however, all internal erosions are not guaranteed to develop into piping. Both observations pose a threat to the safety of the dam and require immediate action, i.e., draining of the reservoir, followed by repairs.

The given background information indicates that internal erosion and piping are closely related but not identical concepts. However, in practice (e.g., ASDSO, 2023b), and in some publications (e.g., Milligan, 2003) they are used interchangeably. In this study, the term "internal erosion" is used for cases that do

2

not progress to piping, and the term "piping" is used for internal erosion that progresses to piping.
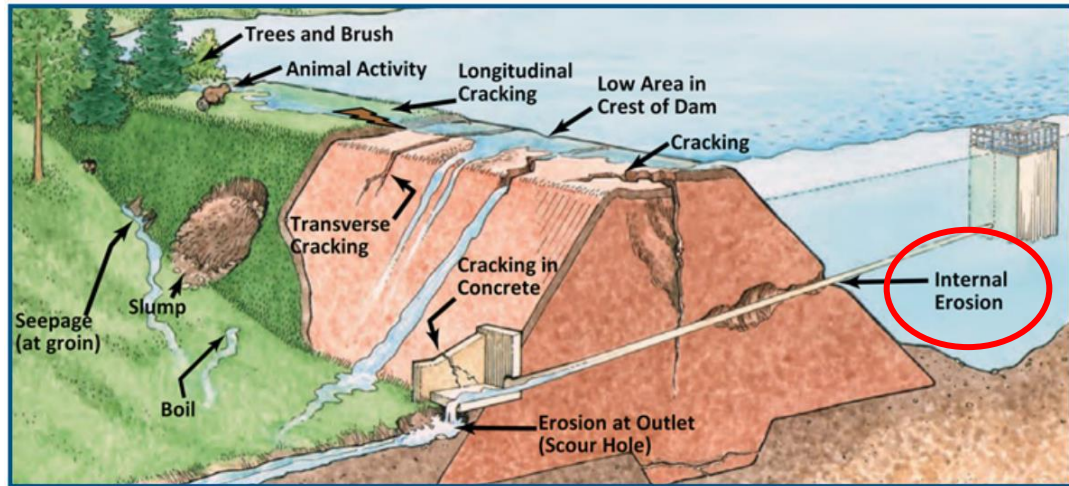
Figure 1.2 Internal erosion and other failure observations in an earthen dam (FEMA, 2016).

Internal erosion is no less important than piping since it is a precursor to piping, and may lead to cracks, cavities, and tunnels weakening the structure and making it susceptible to collapse. Settlements and slope failures may be observed aftermath of internal erosion. In Figure 1.2, the observation labeled "cracking" is due the "internal erosion". The figure illustrates that settlement due to an internal erosion cavity can cause a crack in the dam body, which may propagate to the crest. Additionally, the settlement may cause the crest elevation to lower, resulting in overflow of the reservoir water which may eventually cause a total overtopping failure.

There are some measures aimed at preventing internal erosion. Among those, many common ones are the use of internal filter and seepage collection systems, using properly graded materials that are compacted at the optimum water content, implementation of a properly designed and geologically investigated foundation, and regular inspections and maintenance (ASDSO, 2023a). In earthen dam design, it is crucial to ensure safety against internal erosion. It is also necessary to estimate the probability of occurrence of internal erosion. This study is specifically focused on estimating this probability.

1.2   Literature Review

In past studies regarding the occurrence of internal erosion in earthen dams, the main focus has been on the critical head, H_{crit}, and the critical hydraulic gradient, i_{crit}. H_{crit} is the reservoir head and i_{crit} is the hydraulic gradient that should not be exceeded for safety against internal erosion. Hence, these critical parameters are useful to check for piping probability in earthen dams. The empirical rule suggested by Bligh (1910) for the determination of critical head is considered to be the pioneering study for piping and internal erosion in earthen dams. He suggested that the critical head depends on the base length of the dam and a constant value which is a function of the soil type. Following Bligh's work, other empirical rules, equations, and models were developed for the determination of critical head and critical hydraulic gradient. Considering the equilibrium of forces in the soil, Terzaghi (1929) proposed an equation where the critical hydraulic gradient is defined as the ratio of the buoyant unit weight of soil to the unit weight of the water. Another equation, using a capillary model, was suggested by Khilar et al., (1985) for the critical gradient. In the study, internal erosion was described as a two-step process that consists of particle detachment and particle migration. According to the findings, internal erosion has two possible outcomes, namely particle holdup (plugging) or particle washout (piping), and the outcome depends on the size distribution of migrating particles relative to the pore size distribution of the soil medium. The model used porosity, hydraulic conductivity, and the critical shear stress to determine critical hydraulic gradient. Sellmeyer (1988) suggested that it is important to consider the slit development while computing the critical head since a growing slit may cause piping. The study focused on the equilibrium analysis of forces within the sand boil and slit and proposed an expression for the critical head that uses the median particle size and submerged unit weight of the soil as an input. Ojha et al., (2003a) aimed to evaluate the equations suggested by Sellmeyer (1988) and worked on a critical head model that would provide a theoretical basis for Bligh's work. It was found that the critical head depends on the length of the structure, and soil and fluid properties. The

model developed is capable of reflecting the changes in porosity and the particle size to the critical head. It was concluded that higher values of porosity and particle size result in lower values of length to critical head ratio. This was consistent with Bligh's rules. In a more recent work, Tao (2018) developed a model for the critical hydraulic gradient that is very similar to that of Terzaghi's. Tao's model highlights the effect of friction on the critical hydraulic gradient and uses a particle shape factor in addition to Terzaghi's model. He found that the critical hydraulic gradient required to initiate piping is greater than the gradient determined by Terzaghi's model.

All these models share a common ground in that they use soil properties to determine critical values. Some average soil parameters can be defined over a dam body and used for the calculation of these critical values, however, due to the uncertain nature of soil properties, the average values might be misleading in the internal erosion analysis. Therefore, a stochastic model that considers the probabilistic nature of the soil parameters is needed to better understand the mechanism of internal erosion. To this end, some studies on uncertainties involved in earthen dams and probabilistic-based studies on piping have been carried out. Foster (1999) used an event tree approach to assess the probability of failure of embankment dams by internal erosion and piping. He decomposed the piping process into a series of events and expressed the influence of different factors on each of these events qualitatively. The study found that foundation conditions, soil type, and particle size distribution have an important influence on the probability of piping through the dam body. Milligan (2003) discussed the uncertainties involved in embankment dams and their effects on performance based on case history examples and the author's experience. The study suggested that the capability of engineers to model potential seepage patterns exceeds their capability to control the construction process and account for changes in the site conditions which leads to uncertainties in the behavior of embankment dams. It was also concluded that internal erosion of broadly graded core materials in earthen dams is more likely to occur due to segregation problems when placing these materials. Foster et al., (2000) suggested a method for estimating the piping failure probability of embankment dams based on historic failures and accidents. The

relative influence of factors such as dam zoning, core soil types, filters, compaction, and foundation geology on the likelihood of piping was discussed. Sivakumar Babu & Srivastava (2010) conducted a reliability analysis on rehabilitated earthen dams employing the first-order reliability method. The study considered the variability of the soil shear strength parameters, the horizontal seismic coefficient, and the location of the reservoir at full level. The stability was evaluated in a probabilistic framework. In another study, Redaelli (2011) proposed a method to estimate the probability of breaching by piping through the embankment using personal assessments and evaluations based on subjective experience. The study suggested that piping through the embankment body cannot be studied with the method of reliability analysis since there is a lack of a proper mathematical model. The probability of failure was assessed using some key characteristics of the embankments for several scenarios.

The provided literature indicates that assessment of the probability of internal erosion in earthen dams is challenging due to uncertainties in soil properties and the absence of a suitable probabilistic model to estimate the probability of failure caused by internal erosion, and there is a gap in the literature on this subject matter.

1.3   The Aim and Scope of the Study

The objective of this study is to develop a probabilistic model for determining the probability of internal erosion in the body of an earthen dam. While internal erosion can also occur in the foundation, this study focuses only on the dam body due to the fact that piping-induced failures most commonly occur in this part of the dam (Foster, 1999).

As part of the study, a homogeneous earthen dam with typical fill material was numerically modeled for seepage considering the uncertainty of the soil parameters to determine the hydraulic gradients developing through the dam. In order to check the probability of internal erosion, the critical hydraulic gradient of the soil and the maximum hydraulic gradient developing in the dam body were computed. Monte

Carlo Simulations (MCS) were conducted to generate the probability distribution of the maximum hydraulic gradient, i_{max}. Similarly, a probability distribution of the critical hydraulic gradient was also developed using a random parameter generation algorithm. These two probability distributions were used to calculate the probability of the maximum hydraulic gradient exceeding the critical hydraulic gradient to determine the probability of internal erosion. The results for the homogeneous earthen dam considered were discussed and some protective measures were proposed to decrease the probability of internal erosion. The proposed methodology for the determination of the probability of internal erosion is believed to provide insights for the researchers as well as design engineers working in the industry.

CHAPTER 2

METHODOLOGY

2.1 Seepage through the Dam

Darcy's Law describes the flow through porous media, which can be used to mathematically define the seepage through an earthen dam. In its most general form, this equation is as follows (Papagianakis & Fredlund, 1984; Richards, 1931).

$$\frac{\partial}{\partial x}\left(K_x \frac{\partial h}{\partial x}\right) + \frac{\partial}{\partial y}\left(K_y \frac{\partial h}{\partial y}\right) + \frac{\partial}{\partial z}\left(K_z \frac{\partial h}{\partial z}\right) = S_S \frac{\partial h}{\partial t} \qquad (2.1)$$

In above equation, K_x, K_y, and K_z (m/s) are the hydraulic conductivities in the x, y, and z directions, respectively, S_S (m^{-1}) is the specific storage, h (m) is the water head and t (s) is the time. In the scope of this study, an earthen dam was modeled with a homogeneous fill material. For simplicity, only the maximum cross-section of the dam was considered in the model and a steady flow assumption was made. For two-dimensional steady flow and for homogeneous soil, the groundwater flow equation reduces to the following Laplace equation:

$$K_x \frac{\partial^2 h}{\partial x^2} + K_y \frac{\partial^2 h}{\partial y^2} = 0 \qquad (2.2)$$

The purpose of the numerical model was to solve the above equation for the water head and determine the hydraulic gradient values over the dam body to be used for the estimation of the probability of internal erosion.

The portion of the dam body above the phreatic line is partially saturated, in other words, unsaturated. In this zone, the degree of saturation is less than unity and there

is suction in the soil matrix. Due to suction, some saturated mechanical properties of the soil change, one of which is hydraulic conductivity (Sako & Kitamura, 2006). To determine the relationship between the soil suction and water content, the soil water characteristic curve (SWCC) can be used. These curves can be obtained by experimental methods in which water content and the corresponding suction measurements are plotted and a representative curve is fitted to the data (Lu & Likos, 2004). For the sake of simplicity, instead of plotting a soil water characteristic curve, mathematical functions that are fitted to soil water characteristics data can be used. In the literature, many mathematical models were proposed as representations of SWCC. The three most commonly used models are the Brooks & Corey (1964), Fredlund & Xing (1994), and van Genuchten (1980) model and they are known to successfully estimate the SWCC. A sample SWCC data and the fits generated by these three models are shown in Figure 2.1.
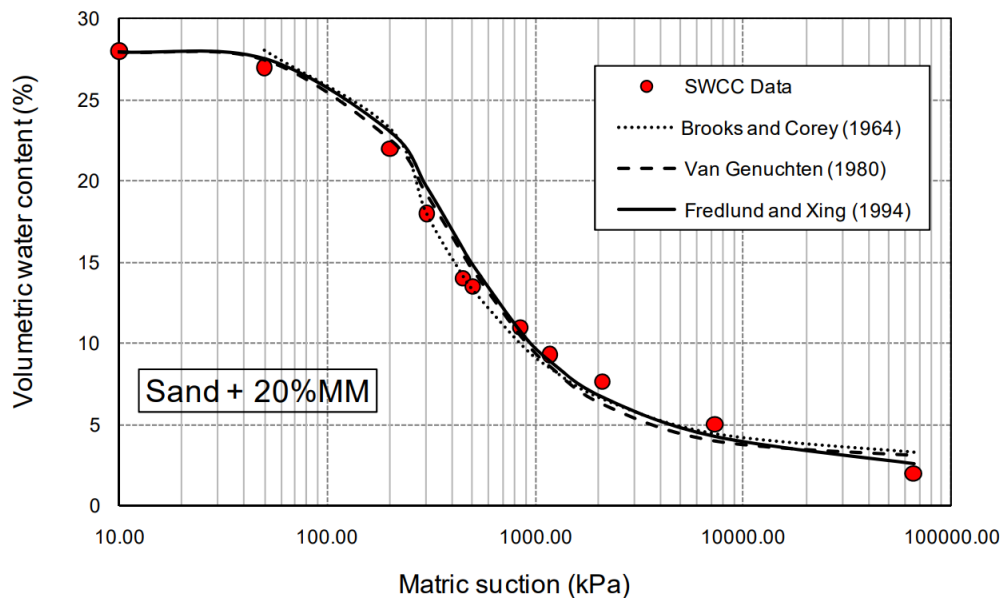
Figure 2.1 Sample SWCC data and the use of three mathematical functions in estimating the curve. This curve is not used in the current study (Reprinted from Pedarla et al., 2012).

For a more accurate estimation of the seepage through an earthen dam, the zone above the phreatic line should also be considered. Therefore, an unsaturated soil

10

model was used to incorporate the seepage through that zone as well in this study. To this end, the van Genuchten (1980) model was adopted. It predicts the unsaturated hydraulic conductivity from soil water content and the saturated hydraulic conductivity. The model provided a relationship between soil water content and suction and defined the following closed-form analytical expression for unsaturated hydraulic conductivity using three parameters, α, n, and m:

$$K_r(p) = \frac{\{1 - (\alpha p)^{n-1}[1 + (\alpha p)^n]^{-m}\}^2}{[1 + (\alpha p)^n]^{\frac{m}{2}}} \qquad (2.3)$$

where, K_r is the relative hydraulic conductivity, which is the normalized form of unsaturated hydraulic conductivity. The variables α, n, and m are curve fitting parameters of the model. Following expression gives the relationship between the variables m and n:

$$m = 1 - \frac{1}{n} \qquad (2.4)$$

The hydraulic conductivity in the saturated and unsaturated zones can be calculated using:

$$K(p) = \begin{cases} K_S K_r(p) & (p < 0) \\ K_S & (p \geq 0) \end{cases} \qquad (2.5)$$

where, K_S (m/s) is the saturated hydraulic conductivity and p (m) is the pressure head. Further details of the model and its parameters can be found in van Genuchten (1980).

2.2   Numerical Modeling of the Seepage

The finite-element method (FEM) was used to solve Eq. (2.2) to numerically model the seepage through the earthen dam. FEM provides an approximate solution for

partial differential equations over a defined geometry. In FEM, the system is subdivided into a number of small, finite number of pieces called elements. This is called the discretization process, and the resulting structure is named the finite-element mesh. Afterward, the partial differential equations are solved over the nodes and elements defined by the mesh using the information provided by boundary conditions.

Solving the governing differential equation of seepage provided the pore water pressures (PWPs) and total heads at nodal points of the finite-element mesh. Subsequent calculations provided the hydraulic gradients, the seepage velocities, and the flow rates. In the scope of this study, Geostudio's SEEP/W™ software (GEOSLOPE International Ltd., 2022) was employed to conduct 2-dimensional finite-element seepage analyses. This software enables the modeling of both saturated/unsaturated and steady/transient seepage under different conditions and has been widely used in practice and for research purposes (Calamak, 2014; Calamak et al., 2017, 2020; Calamak & Yanmaz, 2017, 2018). The software converts the partial derivatives of Eq. (2.1) into integral equations by means of Galerkin's weighted residual method. Further details on the process can be found in GEOSLOPE International Ltd. (2022) and Papagianakis & Fredlund (1984).

Defining the dam material in a numerical simulation is a key step in developing the model especially if the random nature of the soil is considered. The main reason why SEEP/W™ was selected for this study is that it allows the use of add-in functions to define soil properties. Add-in functions eliminate the limitations of the software's interface and provide a broader working environment. These add-in functions are based on Microsoft .NET CLR (Common Language Runtime) and can be created with any programming language that can generate CLR code including C# and Visual Basic .NET (Calamak, 2014). Such add-ins were used in this study to generate the random variables of the soil parameters. The details are provided in Section 2.3.

To model an earthen dam in SEEP/W™, one must define its cross-sectional geometry over the grid space and assign properties of the fill material, such as

hydraulic conductivity, volumetric water content, and porosity, to the geometry polygon. For the upstream face of the dam, a constant water head boundary condition was assigned that represents the reservoir water level and for the downstream face, a seepage face boundary condition was assigned. For the finite-element mesh to be generated over the geometry polygon, an element size must be specified. The mesh size is a crucial factor in modeling as the accuracy of the results is highly dependent on it. Using a coarser mesh size may lead to less accurate results, while an extremely fine mesh would increase the run duration and require more computational power. A basic optimization study is required to save time in modeling, especially if MCS is to be conducted. Such an analysis was undertaken in the scope of the present study and the details are provided in Section 3.1.3.

2.3   Quantifying the Uncertainty

To quantify the random nature of the soil, hydraulic conductivity, K, and van Genuchten's unsaturated flow model parameters, α, and n were randomized throughout the dam body. For this purpose, a probability distribution that represents each variable was determined. The statistics of K of soils has long been studied and it is widely recognized to follow a log-normal distribution (Bennion & Griffiths, 1966; Bulnes, 1946; Law, 1944; Mesquita et al., 2002; Warren & Price, 1961; Willardson & Hurst, 1965). Therefore, K of the fill material was defined as a log-normal random variable. Similar to K, there are uncertainties in fitting parameters of the SWCC as they depend on soil properties. It is suggested that the parameters α and n also follow log-normal distribution for many types of soils (Carsel & Parrish, 1988; Phoon et al., 2010). Therefore, van Genuchten fitting parameters α and n were defined with a log-normal distribution as well. Since the other fitting parameter m is a function of n, it is also log-normally distributed.

In order to define the soil properties as random variables, a random number generation algorithm (Calamak, 2014) was used for all soil properties as an add-in function in SEEP/W™. The code adopts Box-Muller method (Box & Muller, 1958)

for random number generation and uses the probability density functions (PDFs) of variables K, α, and n, defined with a mean and coefficient of variation. Since the variables are log-normally distributed, first their mean and variances are normalized. The normalized forms of the mean and variance are obtained with the following expressions (Ang & Tang, 1975) that are given for hydraulic conductivity as an example:

$$\sigma^2{}_{lnK} = \ln\left(1 + \frac{\sigma^2{}_K}{\mu^2{}_K}\right) \tag{2.6}$$

Then, random values for hydraulic conductivity are computed using the following expression:

$$K = \exp(\mu_{lnK} + \sigma_{lnK}r) \tag{2.7}$$

where r is a random number that is defined by Box-Muller transformation (Box & Muller, 1958):

$$r = (-2lnu_1)^{1/2}sin2\pi u_2 \tag{2.8}$$

where u_1 and u_2 are independent random variables that are obtained from the uniform PDF having the interval of (0,1).

The described random number generation algorithm was used in the properties of fill material as an add-in function. It generated random values for K, α, and n throughout the dam cross-section both in saturated and unsaturated zones. Hence the dam body was modeled as a random domain that represented the uncertainties involved in soil properties.

2.4   Monte Carlo Simulations

In engineering, simulations can be used to predict or study the response of a system using prescribed values for the system parameters. For systems where the input parameters are defined as random variables, MCS can be conducted. This process involves solving the system repeatedly by using randomly generated values for the input parameters, in accordance with the corresponding probability distributions. Mathematical or numerical models can be used as solution tools in this process. The result of this process is a sample of solutions each corresponding to different values of the random input parameters (Ang & Tang, 1984). The typical MCS process is also shown schematically in Figure 2.2.

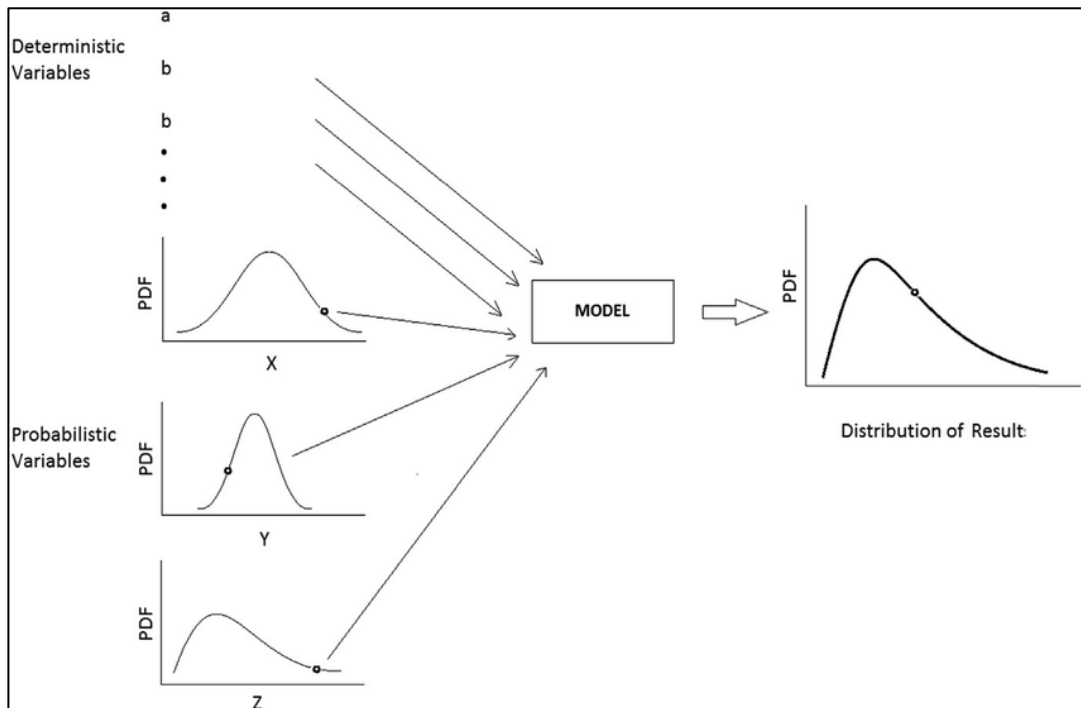Figure 2.2 Monte Carlo simulation diagram (Reprinted from Vu et al., 2018).

MCS is commonly used in engineering to determine the outputs of complex systems. For these systems, a deterministic approach may involve unrealistic assumptions and lead to inaccurate solutions. With MCS, however, systems can be described in detail without using any assumptions or simplifications and can be solved with a

probabilistic approach. Therefore, MCS is the most frequently used method for the stochastic analysis of seepage in porous medium (Kalateh & Kheiry, 2023).

There are other methods used in practice for probabilistic analysis of seepage-related problems, such as perturbation and probabilistic collocation; however, MCS is a simpler and more reliable method. A potential disadvantage of MCS may be the computational effort required for a large number of simulations. However, with the advancements in computer technology, MCS has become a less time-consuming and more powerful tool (Singh et al., 2007).

For the above reasons, the MCS method was adopted for the analysis in this study. The hydraulic conductivity, K, and van Genuchten fitting parameters, α and n were the input parameters that were defined as random variables. For each simulation, random values were generated for K, α, and n from their corresponding PDFs. With each random variable set, seepage analysis was run on SEEP/W™. Since the input parameters were random variables, each run yielded different results. From the results of the desired number of simulations, PDF of the output parameter, i_{max}, was generated.

The number of runs, i.e., simulations, in a MCS is critical and it can have a significant effect on the accuracy and reliability of the results. The number of simulations to be conducted was determined through an optimization process where the variation of the coefficient of variation (COV) of the output is assessed with respect to the varying number of simulations. The details of the determination of the number of MCS are given in Section 3.1.4.

2.5   Estimation of the Probability of Internal Erosion

This study evaluates the probability of internal erosion by computing the probability of the critical hydraulic gradient being exceeded by the existing hydraulic gradients developing throughout the dam body. Therefore, it can be said that the seepage simulations were mainly focused on the determination of the hydraulic gradients

developing over the dam body along both x and y-directions. For the typical conditions of the dam, where the reservoir is at the normal operating level, and for the steady-state flow condition, the critical direction for piping is from upstream to downstream and the gradients developing along the x-direction are comparatively greater than the y-direction gradients. Therefore, only x-direction hydraulic gradients were considered when determining the maximum hydraulic gradient. Then, an adequate number of MCS were conducted and the maximum x-gradient values that exist over the dam body were determined for each simulation. A frequency histogram of the maximum hydraulic gradient was generated, and a probability density function was fitted to the results.

The study uses the critical hydraulic gradient as the limiting parameter for the probability computations. The critical hydraulic gradient is the gradient at which the soil particles start to move. It is a function of the soil properties such as the compaction and the fine material content (Xie et al., 2018) and it is highly uncertain as are other soil parameters. There are some methods and research available to determine the critical hydraulic gradient for a given soil type and/or mixtures. The most widely accepted method was proposed by Terzaghi, (1929):

$$i_{crit} = \frac{\gamma'}{\gamma_w} \qquad (2.9)$$

where γ' (kN/m^3) = buoyant unit weight of soil, γ_w (kN/m^3) = unit weight of the water. Although it is widely used, the above method does not consider the shape and roughness of the soil particles. Another method was proposed by Tao (2018) that accommodates these with a shape factor:

$$i_{crit} = \frac{G_s - 1}{1 + e_0} \left(\frac{SF}{6}\right)^2 \qquad (2.10)$$

where G_S = Specific gravity, e_0 = Initial void ratio, SF = Shape factor.

These two methods were used in the study for critical hydraulic gradient calculations. As it is highly uncertain, the soil parameters included in these models were defined

as random variables with representative probability distributions. A random number generation algorithm was used to populate the input parameters in Eqs. (2.9) and (2.10) and the same number of critical hydraulic gradient values are generated as the number of MCS conducted for the seepage through the earthen dam and for the determination of the maximum hydraulic gradient.

The last step is to determine the probability of the maximum hydraulic gradient exceeding the critical values. Figure 2.3 shows the probability density functions of two random variables, namely demand (shown with "S" in the figure) and the resistance (shown with "R" in the figure). The shaded area represents the probability of one variable exceeding the other and when it is calculated, one can determine the probability of R exceeding S. This probabilistic method was applied to the effective problem of the study. To do so, the probability distribution functions of both the critical and maximum hydraulic gradients were derived. For this purpose, curve-fitting studies were conducted to find the best distribution type that represents the generated frequency histograms of the parameters. As a result, a similar chart to the figure was generated for i_{max} and i_{crit}, which are represented with S and R, respectively, in the figure.
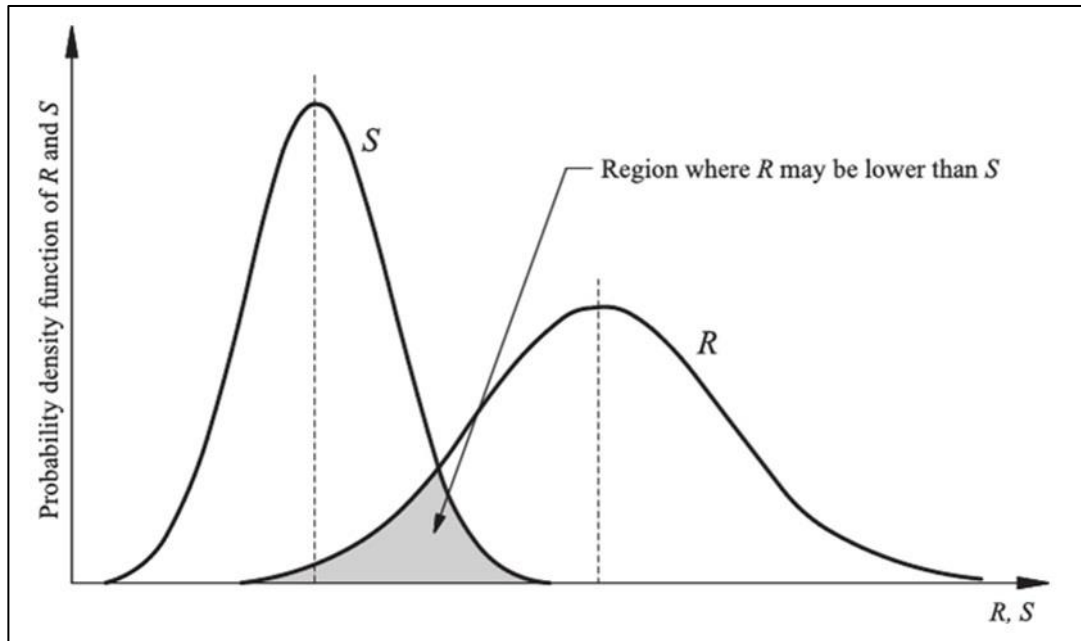
Figure 2.3 Probability of exceedance for two random variables (Reprinted from Fernandes, 2020).

The computation of the probability of exceedance for two random variables is a straightforward process when both variables follow a normal or log-normal distribution. However, when the variables follow different types of distributions, computing this probability by simple hand calculations is difficult and time-consuming. In order to calculate exceedance or failure probabilities in complex systems where the random variables follow different types of distributions, one of the First Order Reliability Method (FORM), First Order Second Moment Method (FOSM), or Mean Value First Order Second Moment method (MVFOSM) methods can be used. Reliability Index Calculator (RIC) (Yücemen, 2021), is a software that adopts these methods and computes the reliability index, β, a quantitative representation of reliability, and the probability of failure of a system and was adopted in this study to estimate the probability of i_{max} exceeding i_{crit}. The software used three input files that were prepared in text format and they were namely .b, .g, and .dgdx extension-files. The .b extension-file was the main input file where the random variables involved in the system were defined with the information of their

corresponding distributions and distribution parameters. In addition, the methods that were used for the reliability analysis such as First Order Reliability Method (FORM), First Order Second Moment Method (FOSM), and Mean Value First Order Second Moment method (MVFOSM) were specified in .b file. In the study, FORM was used for the probability computations. In the .g file, the limit state function was defined. The limit state function, g, is a function defined with the variables involved in the system. It takes values above zero for when the system is safe and below zero for when the system is in failure condition. In reliability analysis, the gradient of the limit state function was also used and RIC software requires this information as an input. The gradient of the limit state function was specified in the .dgdx file. After defining all input files, the reliability analysis was conducted with the executable file of the software. Results of the analysis for all methods specified in the .b file were given in an output file that includes the reliability indices and probability of failure of the system. For determining the probability of i_{max} exceeding i_{crit}, the following limit state function and its gradients were used.

$$g(x) = i_{crit} - i_{max} \tag{2.11}$$

$$\frac{dg}{dx}(i_{crit}) = 1 \tag{2.12}$$

$$\frac{dg}{dx}(i_{max}) = -1 \tag{2.13}$$

where $g(x)$ is the limit state function and dg/dx is the gradient of the limit state function.

CHAPTER 3

APPLICATION PROBLEM AND THE RESULTS

3.1   Application Problem

The proposed methodology was applied to the stochastic analysis of the 2-dimensional, steady, saturated and unsaturated flow of an earthen dam. The problem description, soil properties, and the details of the numerical model are provided in this section.

3.1.1   Description

The analyses were conducted for a hypothetical homogeneous earthen dam that was previously investigated for a stochastic seepage analysis (Calamak & Yanmaz, 2017). The dam had a height of 25 m and a crest width of 8 m. The upstream and downstream slopes of the dam were 1V:3.0H and 1V:2.0H, respectively. The reservoir water depth of the dam was 23 m, and it was assumed to be constant. The dam cross-section is given in Figure 3.1.
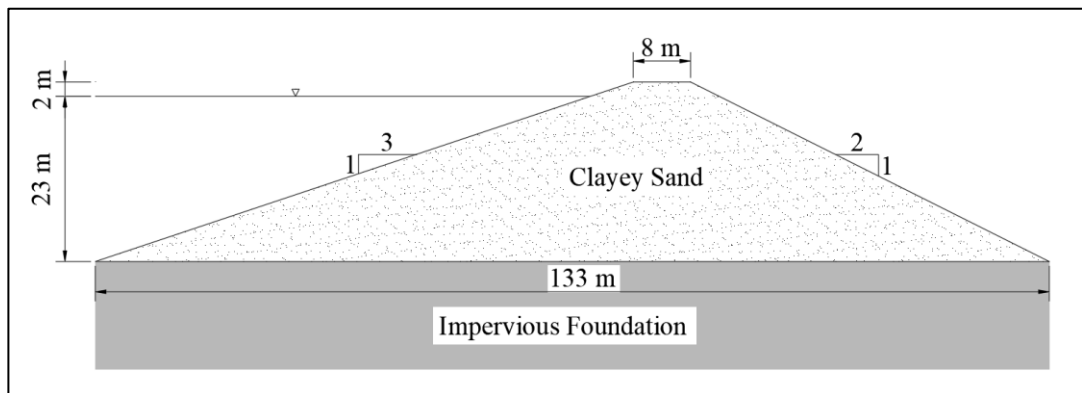

Figure 3.1 The cross-section of the earthen dam under investigation.

3.1.2 Material and the Boundary Conditions

Since the dam under investigation was a homogeneous dam, a single material was used for the fill: clayey sand. The main parameter that defined the fill material was the saturated hydraulic conductivity, K_S, since it is the governing factor in the seepage and in the solution of the differential equation of the flow (see Eq. (2.2)). For the fully saturated zone of the dam, where the soil pores are completely filled with water, K_S is the only parameter that was used. For the zone above the phreatic line of the seepage, in other words, the unsaturated zone, the van Genuchten method parameters α, n, and m were used together with K_S to estimate the unsaturated hydraulic conductivity.

Using these values and their probability distributions, the algorithm generated random values for the input parameters. The mean and COV values for the hydraulic conductivity and for the van Genuchten parameters were directly obtained from SoilVision (Fredlund, 2005), a comprehensive database system for the properties of soils, whether they are saturated or unsaturated, for clayey sand. The mean and COV for each input parameter are given in Table 3.1. All input parameters followed the log-normal distribution.

Table 3.1 Mean and the coefficient of variation of input parameters.

Input Parameter	Mean	COV
K_S	1.03×10^{-5} m/s	2.09
α	0.28	0.63
n	1.23	0.08

After the properties of each input parameter were defined, the fill material was assigned to the dam geometry. Figure 3.2 shows the FEM model of the dam body along with the boundary conditions of the numerical model. The upstream boundary condition was determined by the reservoir head and was defined in the numerical model as a constant head boundary condition of 23 m, while the potential seepage face boundary condition was used for the downstream side. The foundation is considered to be impervious, and a no-flow boundary condition is assigned for this region.
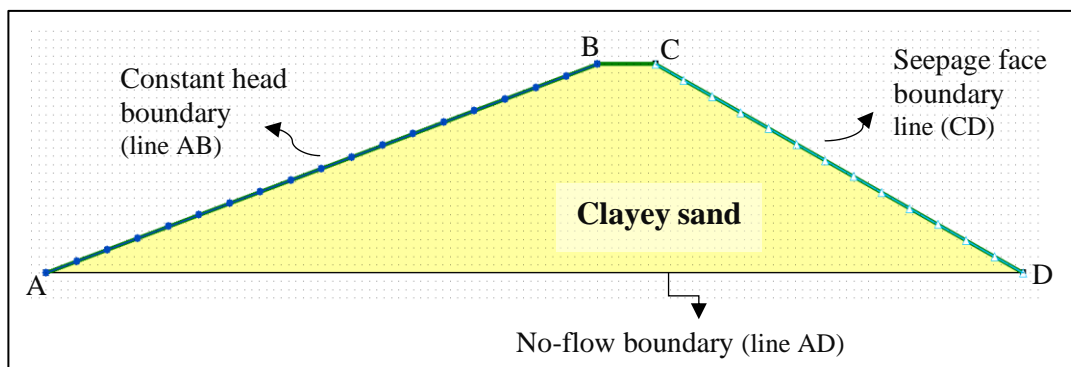

Figure 3.2 The finite-element model of the dam and the boundary conditions.

3.1.3 The Finite-element Mesh

The element/mesh type and size in FEM is a user-defined variable in SEEP/W™. The mesh size is controlled by the global element size. The global element size is a constraint that determines the maximum possible mesh element edge size. The mesh was generated over the dam body with a pattern formed by quadrilaterals and triangles for various element sizes. Using quadrilaterals for the mesh pattern reduces the approximation error and the number of elements in the mesh (Bommes et al., 2012). Triangles were also used to follow the geometry changes better. The resulting meshes are shown in Figure 3.3-Figure 3.6 for various global element sizes.

Figure 3.3 Finite-element mesh created with a global element size constraint of 5 m.

Figure 3.4 Finite-element mesh created with a global element size constraint of 2.5 m.
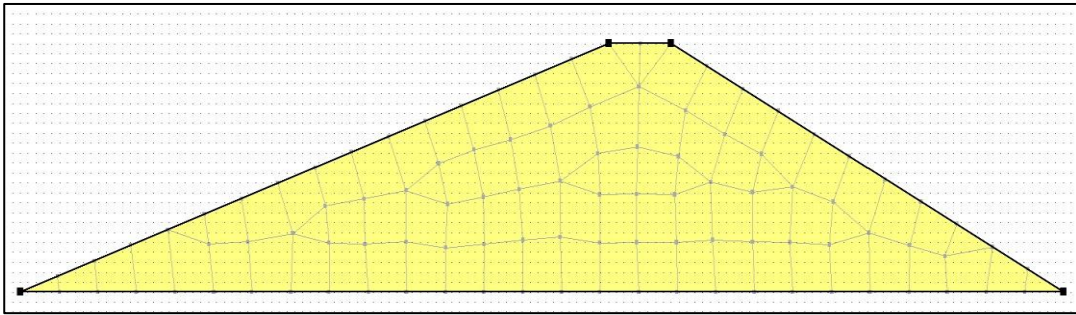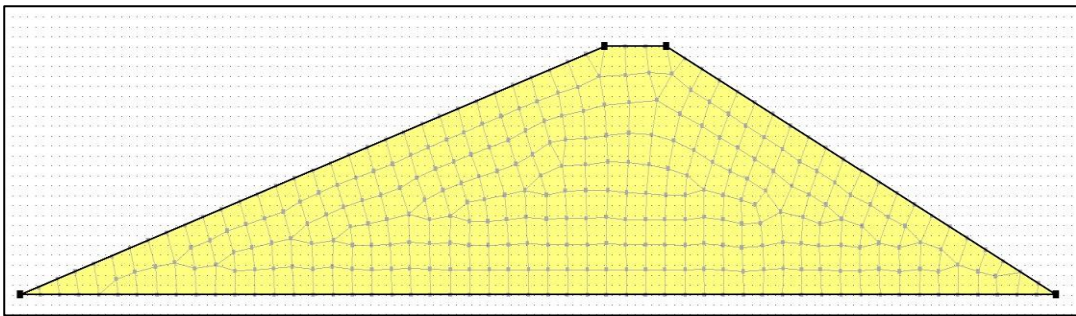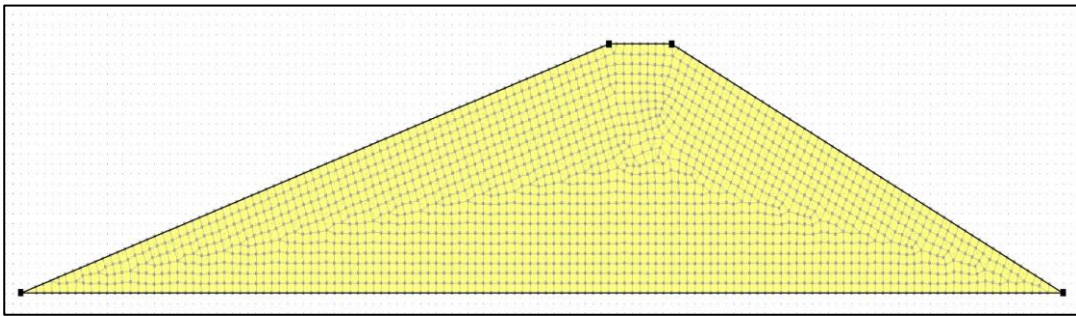

Figure 3.5 Finite-element mesh created with a global element size constraint of 1 m.
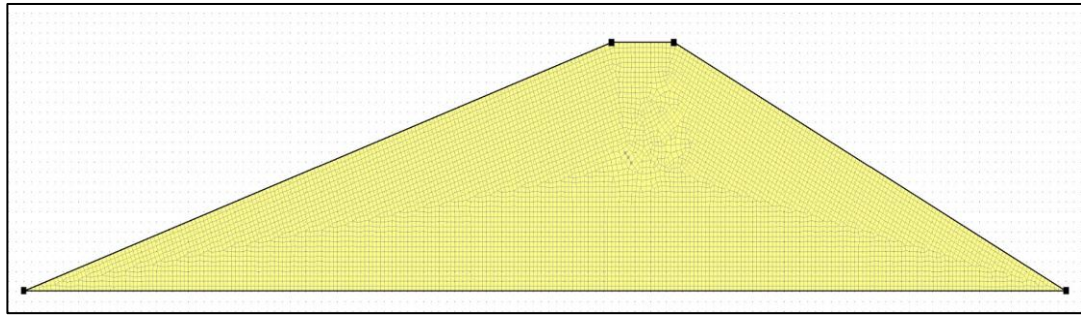
Figure 3.6 Finite-element mesh created with a global element size constraint of 0.5 m.

Considering that the differential equations are solved at the nodes and elements of the finite-element mesh, it is obvious that a smaller mesh size provides more precise and accurate results over the defined geometry and a better representation of the system. However, as the mesh size decreases, generation of the finite-element mesh gets more difficult, and it requires more computational power. The solution becomes a more and more time-consuming process. Therefore, a mesh size optimization study was conducted in the study. The purpose of this study was to find a mesh size that provides a high level of accuracy in the solution while having an acceptable amount of computational load. The study was conducted on a deterministic model of the application problem. The soil of the fill material was defined with constant properties, i.e., constant K. For the sake of simplicity, the seepage analysis was conducted using only a saturated soil model. Therefore, van Genuchten parameters, α, n, and m were not used for this particular analysis. Since the only purpose of this study was to determine the optimum mesh size to be used for the MCS and the probabilistic analysis, the simplifications were assumed to be acceptable. The deterministic value for K was assumed to be the mean of the parameter given in Table 3.1. The mesh size optimization study was conducted by performing deterministic seepage analysis on the described model for global element sizes of 0.15 m, 0.20 m, 0.25 m, 0.30 m, 0.40 m, 0.50 m, 0.75 m, 1.00 m, 1.50 m, 2.00 m, 2.50 m, 3.00 m, 3.50 m, 4.00 m, 4.50 m, and 5.00 m. For each analysis, the x-, y- and xy-gradients were determined for a preselected point which was located at (90,10) of a coordinate system whose origin passes through the heel of the dam. Figure 3.7 shows the

coordinate system and the preselected control point for the mesh size optimization study. This location was randomly selected at a region close to the downstream face of the dam since this area was more susceptible to the initiation of internal erosion and the results of the seepage analysis might prove to be more important for the model.
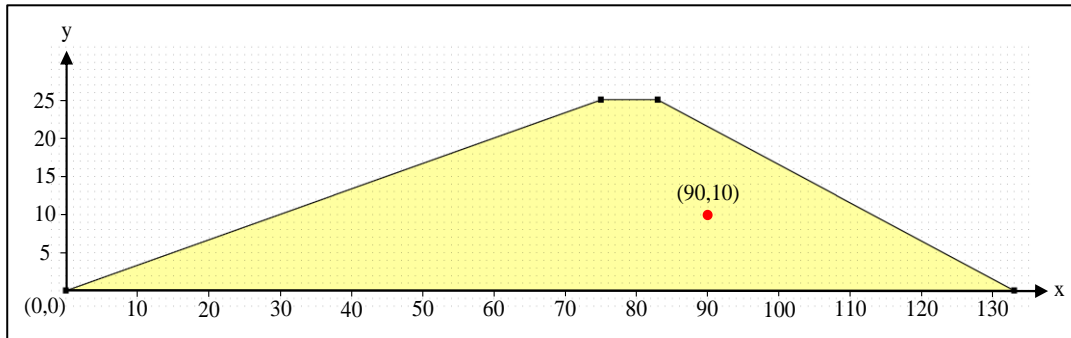
Figure 3.7 Preselected point used in the mesh size optimization study.

For values below the global mesh size of 0.15 m, the mesh generation process took a very long time, and it caused the program to freeze completely for a computer with a 4-core, 4 GHz processor and 16 gigabytes of RAM. The numerical solution to the problem took about 15 seconds when the mesh size was 5.0 m, and it took around 3 minutes if the mesh size was 0.5 m with the aforementioned computer processor and memory features. Table 3.2 shows the hydraulic gradients at the preselected point and the total number of nodes and elements generated for the selected element sizes. The variations of the gradients at the control point with respect to mesh size are presented in Figure 3.8-Figure 3.10.

Table 3.2 Discretization details and gradients at the preselected point for different mesh sizes.

| Global element size (m)	Number of nodes	Number of elements	x-gradient	y-gradient	xy-gradient
5.0	102	79	0.246	-0.050	0.251
4.5	123	97	0.239	-0.066	0.248
4.0	147	118	0.244	-0.064	0.253
3.5	184	151	0.238	-0.052	0.244
3.0	245	207	0.232	-0.066	0.241
2.5	330	284	0.235	-0.054	0.241
2.0	520	461	0.241	-0.056	0.248
1.5	871	794	0.239	-0.059	0.246
1.0	1905	1788	0.236	-0.058	0.243
0.75	3303	3152	0.238	-0.060	0.246
0.50	7299	7071	0.237	-0.059	0.244
0.40	11317	11042	0.238	-0.059	0.245
0.30	19697	19352	0.237	-0.060	0.245
0.25	28210	27805	0.237	-0.060	0.245
0.20	43379	42903	0.237	-0.060	0.245
0.15	74798	74335	0.237	-0.060	0.245
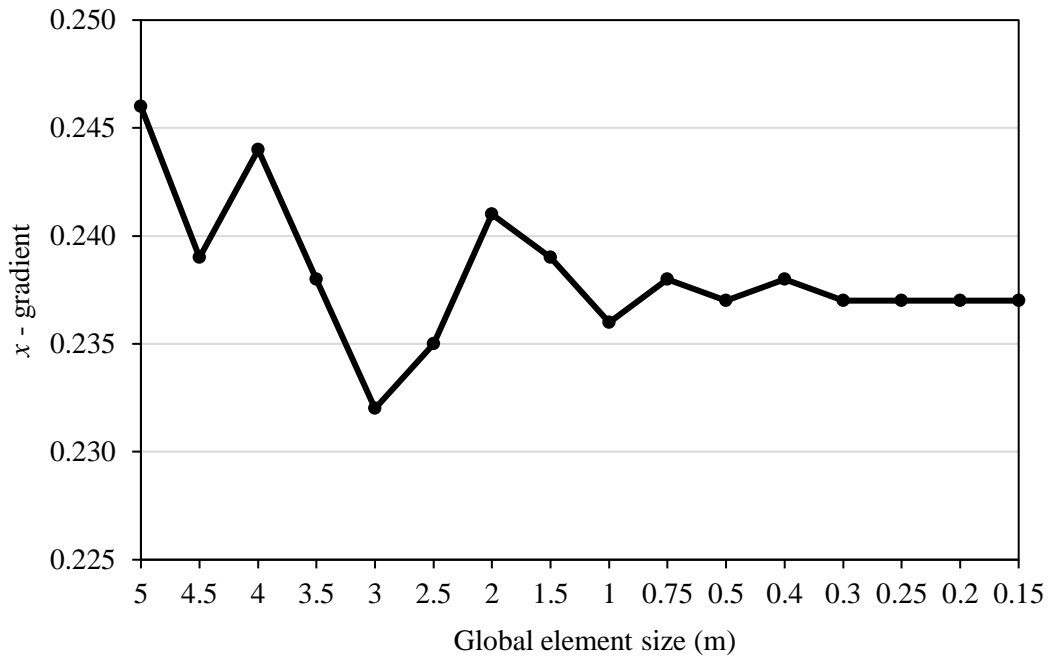
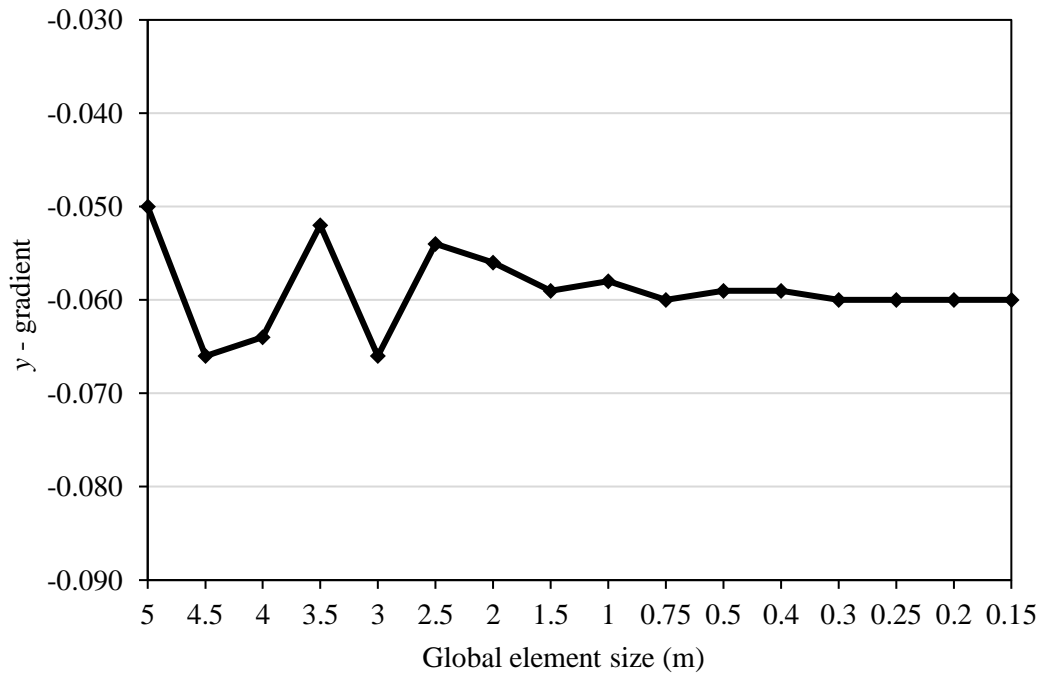Figure 3.8 *x*-gradient at the preselected point for varying global element sizes.

Figure 3.9 *y*-gradient at the preselected point for varying global element sizes.
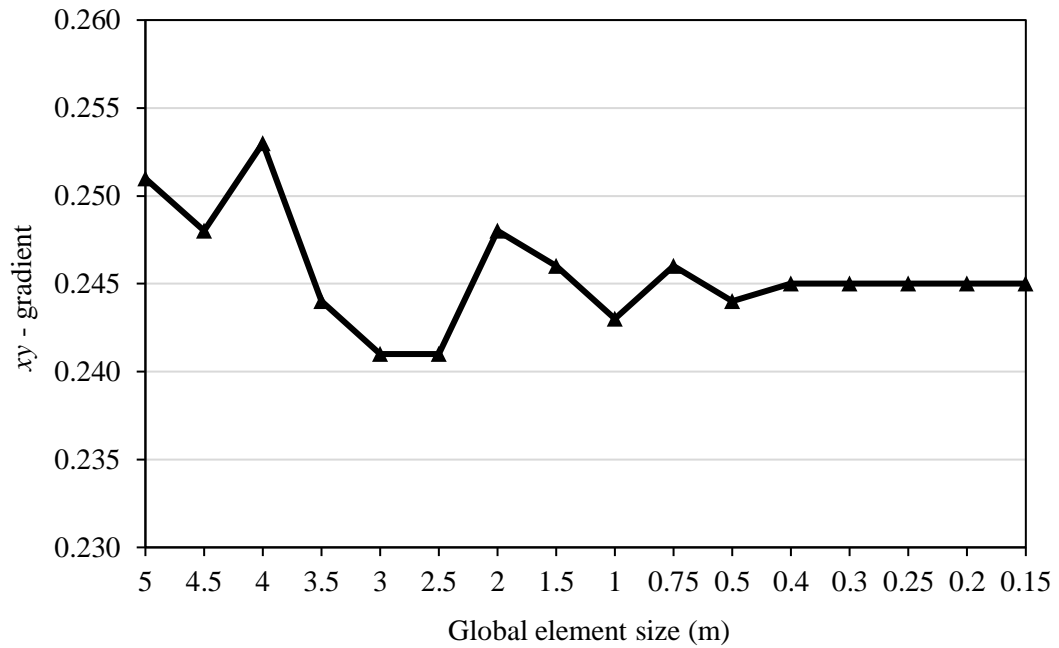
Figure 3.10 *xy*-gradient at the preselected point for varying global element sizes.

The results show that there was not a significant change in the gradients for element sizes less than 1.0 m and below at or around 0.5 m the values converge to a single value. Therefore, the biggest element size that gives the most precise solution is 0.5 m and the optimum element size was selected as 0.5 m.

3.1.4   The Number of Monte Carlo Simulations

There are no theoretical guidelines for the required number of MCS in a study. However, with more simulations, the standard deviation of the resulting data decreases since it is inversely related to the sample size. This means Monte Carlo experiments yield more precise results with more simulations (Mooney, 1997).

In this study, the adequate number of simulations was determined by checking the COV of the output parameter, namely the maximum hydraulic gradient, for various number of simulations. It can be said that when the COV of i_{max} stabilizes, the number of simulations is adequate. Figure 3.11 shows the variation of COV of i_{max} with respect to the number of simulations.
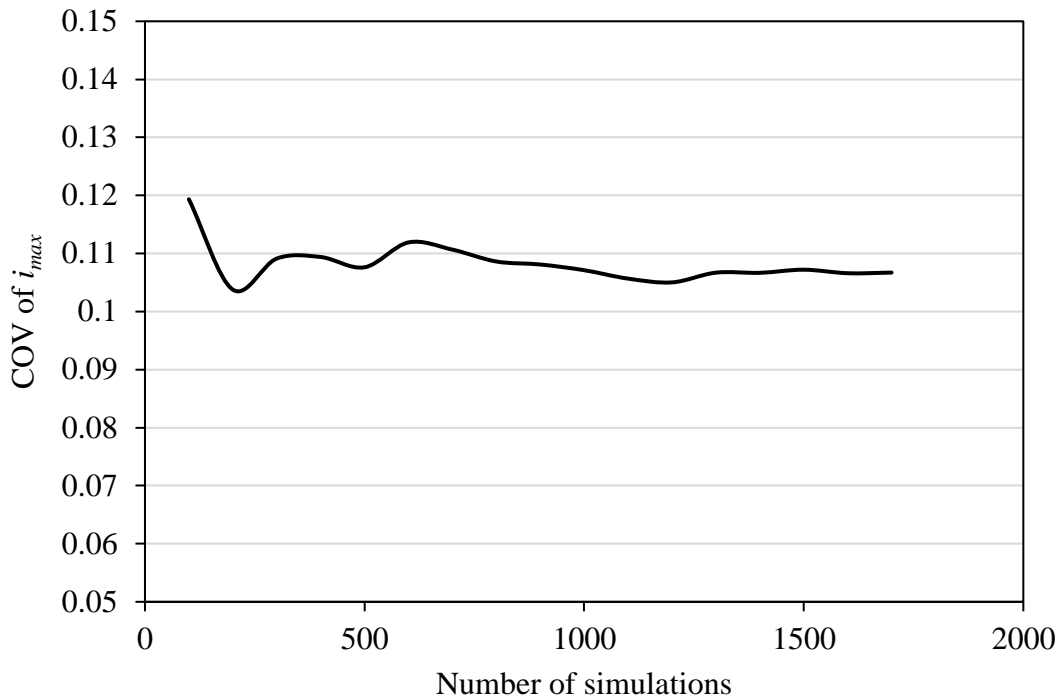
Figure 3.11 The change of coefficient of variation of the maximum hydraulic
gradient with respect to the number of MCS.

The COV of i_{max} stabilizes after approximately 1300 simulations. Accordingly, any number of simulations above this value yielded precise results. To be on the safe side, the number of MCS runs was selected to be 1500 simulations in the study and the same number of i_{max} were generated for determination of its probability density function.

3.2   The Results

Before presenting the probabilistic analysis results, for a better understanding of the uncertainty of the soil parameters and its effects on hydraulic gradients throughout the dam, the hydraulic conductivity distribution for an example MCS run is presented in Figure 3.12. Here in the figure, the contour lines where the hydraulic conductivity had the same value are shown with a color scale in which the green shows lower hydraulic conductivity and orange shows the higher. As can be seen in the figure, K was randomly dispersed throughout the soil body, just as real-world soil would be.
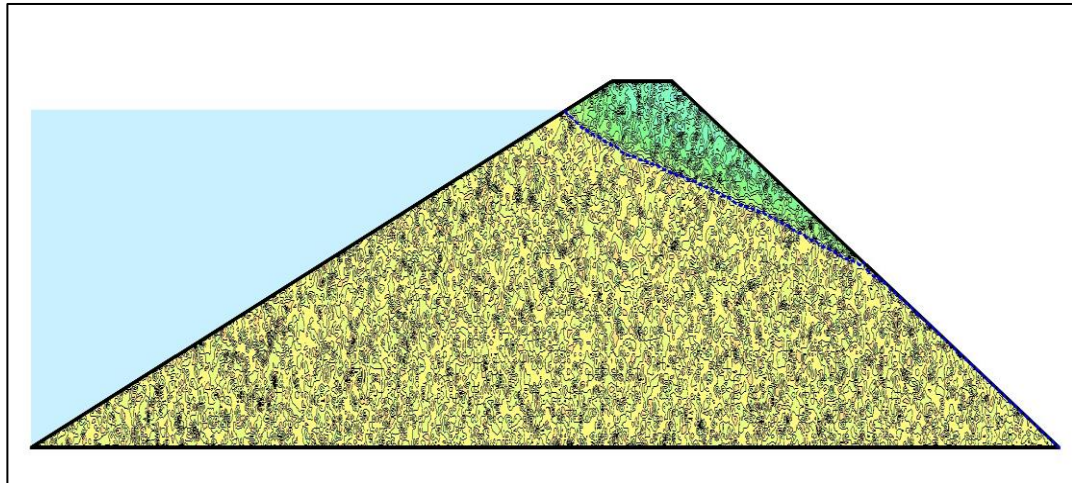
Figure 3.12 Contour lines of randomly generated hydraulic conductivity in the *x*-direction. The vertical scale is distorted for a better understanding of the distribution.

Since the parameters used to define the soil were random variables, the behavior of the dam body was expected to be completely different from that of a deterministic model of the dam. The randomness of the input variables had to be reflected in the hydraulic gradients. Therefore, similarly, the distribution of the hydraulic gradients along *x*-direction, i.e., *x*-gradients was derived for the same case given in Figure 3.12 and presented in Figure 3.13. In this figure, as in the previous figure, the *x*-gradient contour lines are shown with a color scale where blue and green colors represent lower values and yellow and orange colors represent higher values of the gradient. The erratic distribution of hydraulic gradient over the dam body can be observed from the results. Additionally, the phreatic line of the seepage, where the pressure is atmospheric and the saturated and unsaturated soil zones are divided, is shown with the blue dashed line. Since the phreatic line reached the downstream face, it can be concluded that the dam might be susceptible to internal erosion and the probability of occurrence of it should be investigated.
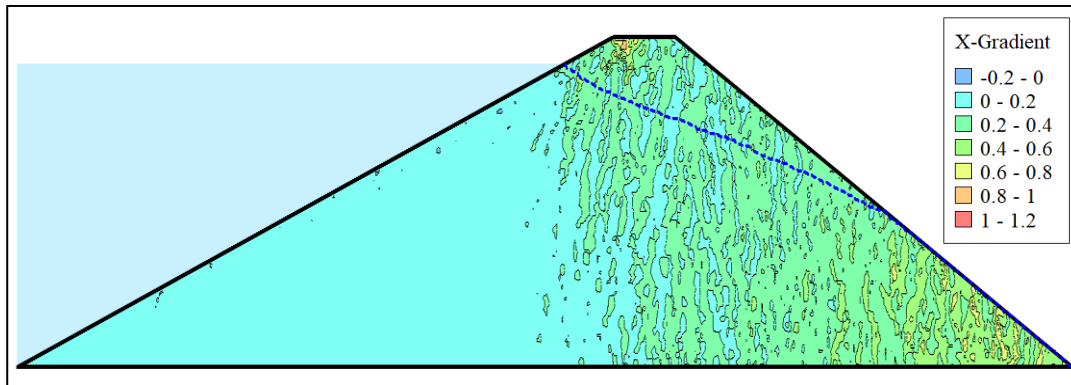
Figure 3.13 The *x*-gradient contour lines for a random MCS run. The vertical scale is distorted for a better understanding of the distribution.

It was realized from Figure 3.13 that there was a region near the crest of the dam where very high values of hydraulic gradient occurred. Several other hundreds of MCS runs also yielded similar results for the same region. A close-up view of the case is presented in Figure 3.14. This zone was expected to be always partially saturated, i.e., unsaturated since it was elevated above the reservoir water level and was not susceptible to internal erosion. Therefore, the hydraulic gradients from this region were disregarded in the probability computations.

Figure 3.14 The crest region exhibiting high hydraulic gradient values. This is observed in several hundreds of MCS runs.

3.2.1 The Frequency and Probability Distribution of the Maximum Hydraulic Gradient

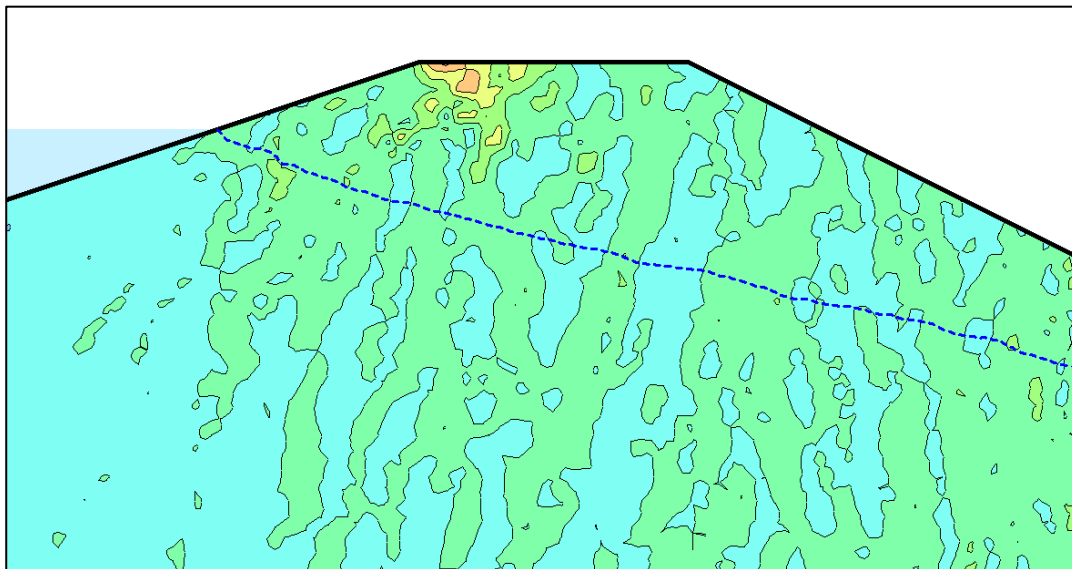MCS yielded 1500 sets of seepage results including pore water pressures and total heads at nodal points, seepage velocities, hydraulic gradients, etc. The hydraulic gradients were further processed to reveal the probabilistic structure of the variable. To this end, the maximum hydraulic gradient values that exist throughout the dam body were retrieved for each MCS run and statistically analyzed. A frequency histogram was generated for i_{max} and it is given in Figure 3.15. In addition, in Table 3.3 the mean, standard deviation, and COV of the i_{max} are presented. According to the results, i_{max} exhibited values ranging from 1.0 to 2.0. Its distribution followed a right-skewed trend with a mean value of 1.32, a standard deviation of 0.14, and a COV of 0.11.
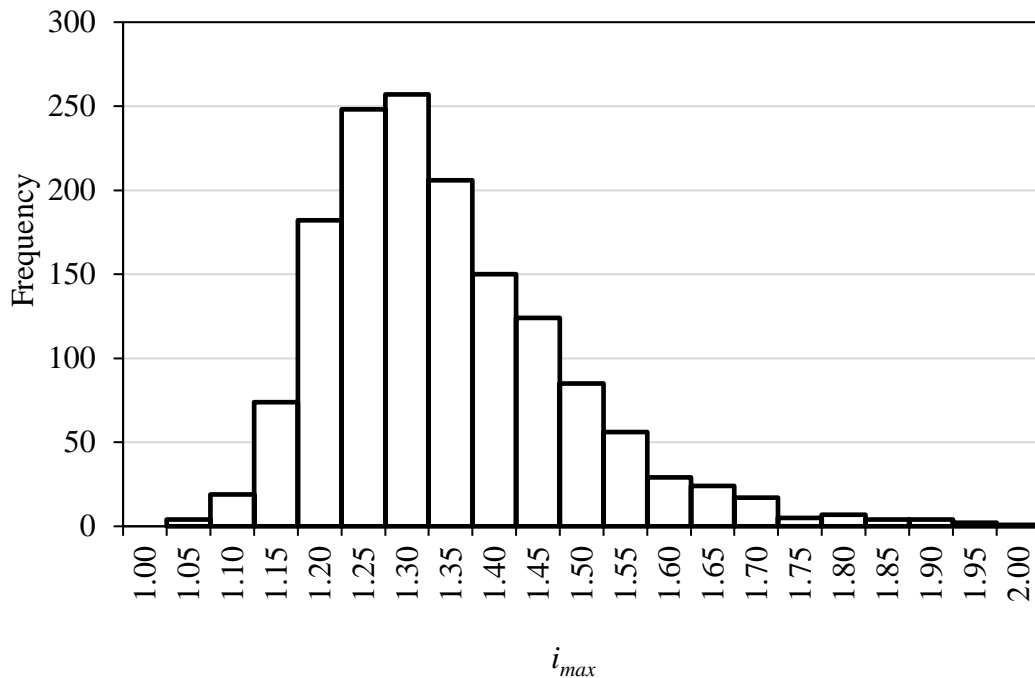

Figure 3.15 The frequency histogram of i_{max} for 1500 MCS.

Table 3.3 Mean, standard deviation, and coefficient of variation of i_{max} for 1500 MCS.

Parameter	Mean	Standard Deviation	COV
i_{max}	1.319	0.141	0.107

3.2.2 The Frequency and Probability Distribution of the Critical Hydraulic Gradient

To generate the probability distribution for the critical hydraulic gradient, the same number of MCS were performed on the critical hydraulic gradient models suggested by Terzaghi (1929) and Tao (2018), the details of which were given in Section 2.5. The random soil input parameters were the buoyant unit weight, γ' for Terzaghi's model, and specific gravity, G_S and initial void ratio, e_0 for Tao's model. Warrick & Nielsen (1980) notes that log-normal distribution is often observed for e_0 whereas γ' and G_S follow a normal distribution (USBR, 1987). The data statistical properties of these random variables obtained from SoilVision (Fredlund, 2005) database for clayey sand are given in Table 3.4.

Table 3.4 Statistical properties of the random input parameters of i_{crit}

Soil Parameter	Mean	Standard Deviation	COV
γ'	9.63 kN/m^3	1.26 kN/m^3	0.13
G_S	2.69	0.13	0.05
e_0	0.74	0.19	0.26

In addition, there were deterministic input parameters in both models. The unit weight of water, γ_w in Terzaghi's model was taken as 9.81 kN/m^3 and the shape

factor, SF in Tao's model was taken as 6.1, assuming rounded particles, according to the values suggested by Fair and Hatch (Fair et al., 1933).

MATLAB codes were written to run simulations for both aforementioned models. In order to generate random numbers for the input parameters given in Table 3.4, *normrnd* and *lognrnd* functions are used for the variables that follow normal and lognormal distributions, respectively. These functions use Marsaglia polar method (Marsaglia & Tsang, 1984) to generate random numbers. The MATLAB codes can be found in the Appendix. The frequency histogram was generated for i_{crit} for 1500 simulations, and they are given in Figure 3.16 and Figure 3.17 for Terzaghi's and Tao's models, respectively. Additionally, the mean, standard deviation, and COV for the i_{crit} are provided in Table 3.5. The simulation results using both models indicated that i_{crit} showed values ranging from 0.6 to 1.5 with a mean value of around 1.00, a standard deviation of 0.13, and a COV value of 0.13. The distribution shapes of i_{crit} were very similar for the two models; they are visually symmetrical around the mean value, having a proper peak, and tails extending towards the ends with a bell-shaped curvature.
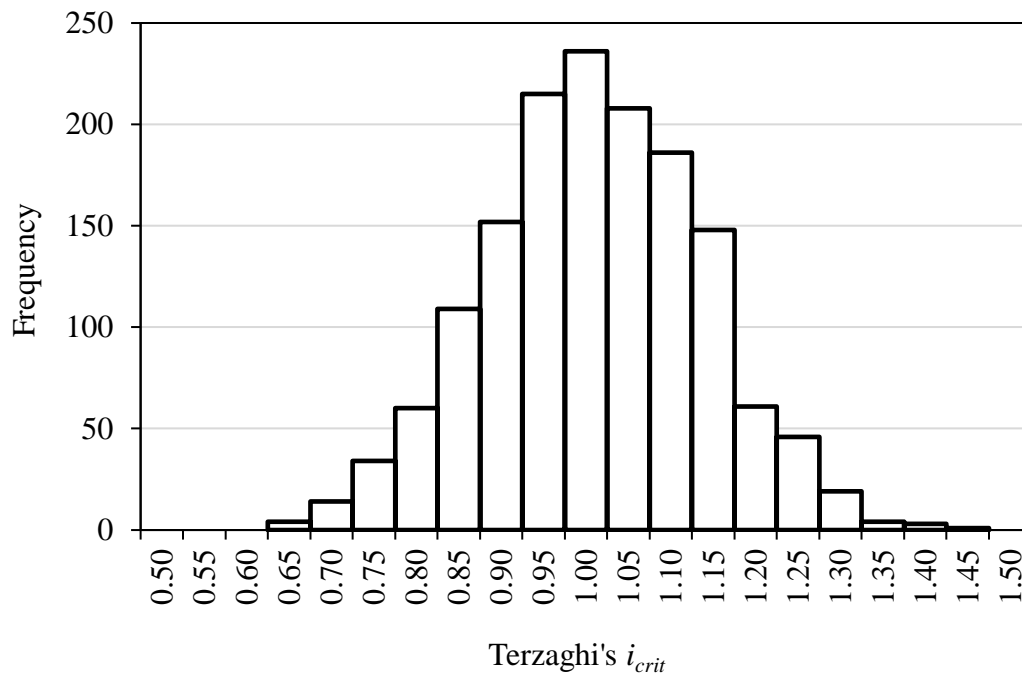
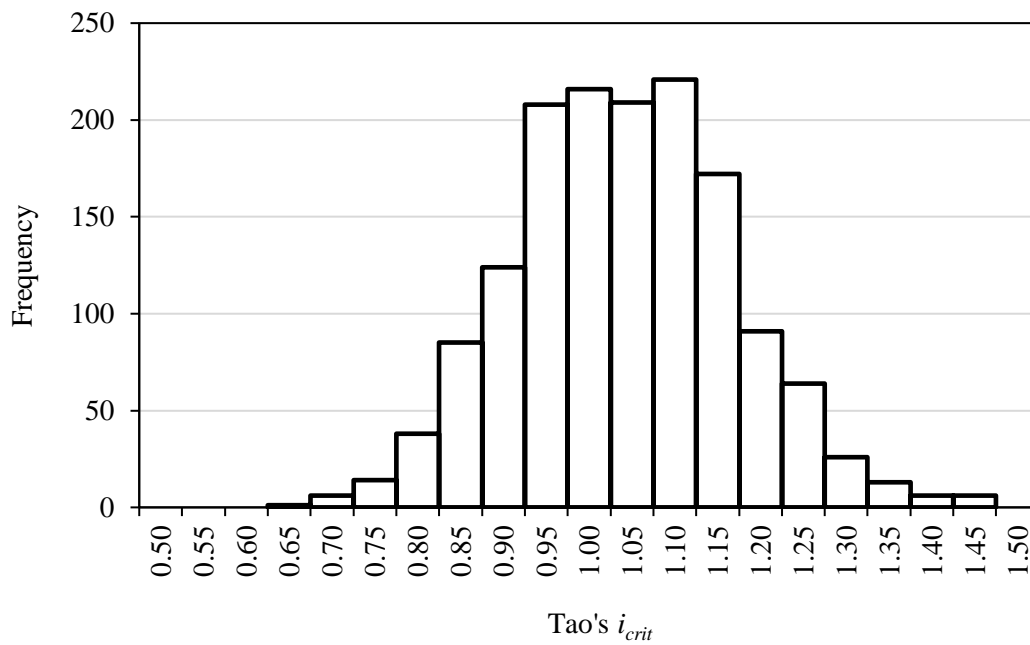Figure 3.16 The frequency histogram of Terzaghi's i_{crit} for 1500 MCS.

Figure 3.17 The frequency histogram of Tao's i_{crit} for 1500 MCS.

Table 3.5 Mean, standard deviation and coefficient of variation of i_{crit} for 1500 MCS.

Parameter	Mean	Standard Deviation	COV
Terzaghi's i_{crit}	0.985	0.127	0.13
Tao's i_{crit}	1.016	0.127	0.13

3.2.3   Distribution Fitting

In order to calculate the probability of i_{max} exceeding i_{crit}, the probability distributions of these two parameters must be known. To find the distributions that best represent i_{crit} and i_{max}, a distribution fitting study is performed. For this purpose, Chi-square and Kolmogorov Smirnov goodness of fit tests (Ang & Tang, 1975) were performed on the sets of i_{max} and i_{crit} in MATLAB. In the distribution fitting study, two commonly used probability distributions in statistical modeling were used: normal and log-normal distributions. If these two were not able to statistically identify the set of variables, a probability distribution that is common for statistically defining the seepage through earthen dam parameters, namely the generalized extreme value (GEV) distribution (Calamak, 2014) was tested for fitting. The results of the goodness of fit tests are given in Table 3.6.

Table 3.6 The goodness of fit test results for Tao's and Terzaghi's i_{crit}, and i_{max}.

Parameter	PDF Type	Chi-square test decision	Kolmogorov Smirnov test decision
Terzaghi's i_{crit}	Normal	Accept	Accept
	Lognormal	Reject	Reject
Tao's i_{crit}	Normal	Accept	Accept
	Lognormal	Reject	Reject
i_{max}	Normal	Reject	Reject
	Lognormal	Reject	Reject
	GEV	Accept	Accept

According to the results, i_{crit} of both models followed a normal distribution, whereas i_{max} followed the GEV distribution. Figure 3.18-Figure 3.20 show the fitted PDFs on the i_{crit} and i_{max} frequency histograms. It can be seen from the figures that the distribution curves were visually close to the histograms, which was an indicator of the validity of the goodness of fit tests.
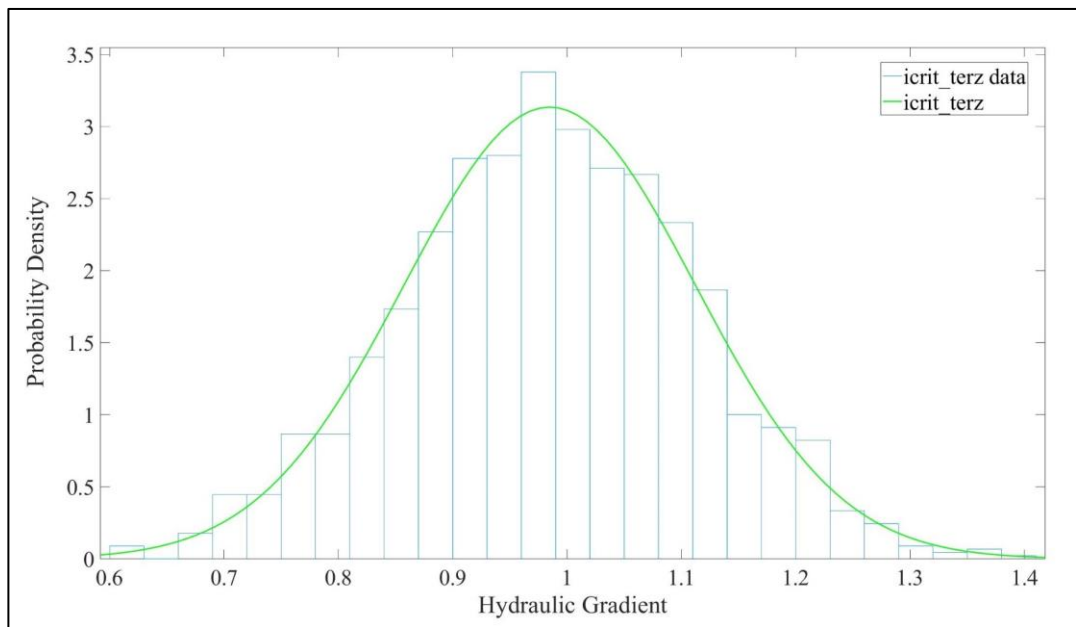
Figure 3.18 Normal distribution fit on Terzaghi's i_{crit} data
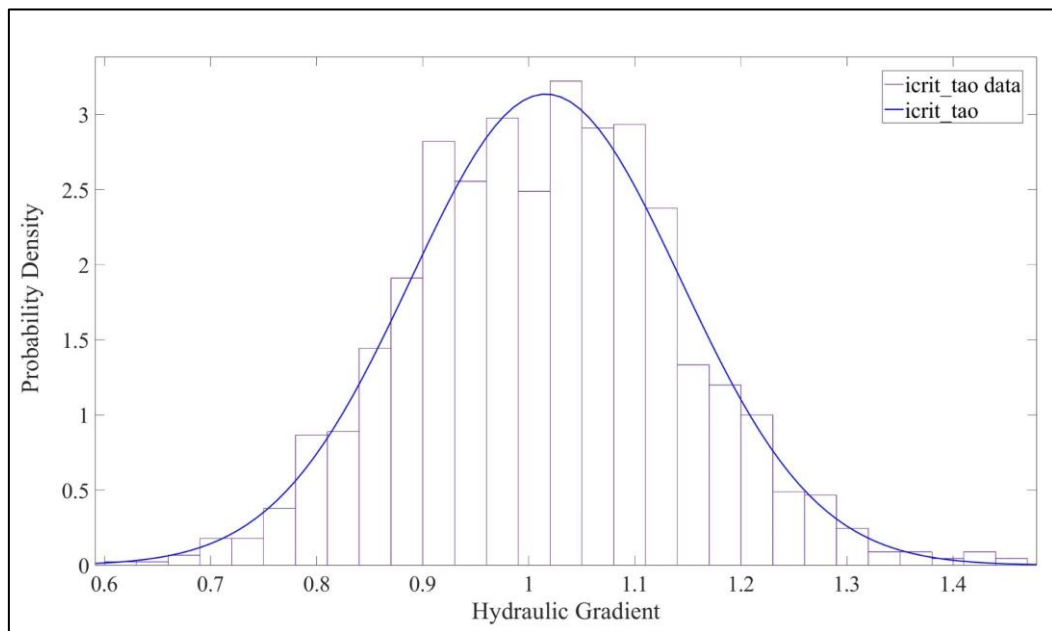
Figure 3.19 Normal distribution fit on Tao's i_{crit} data
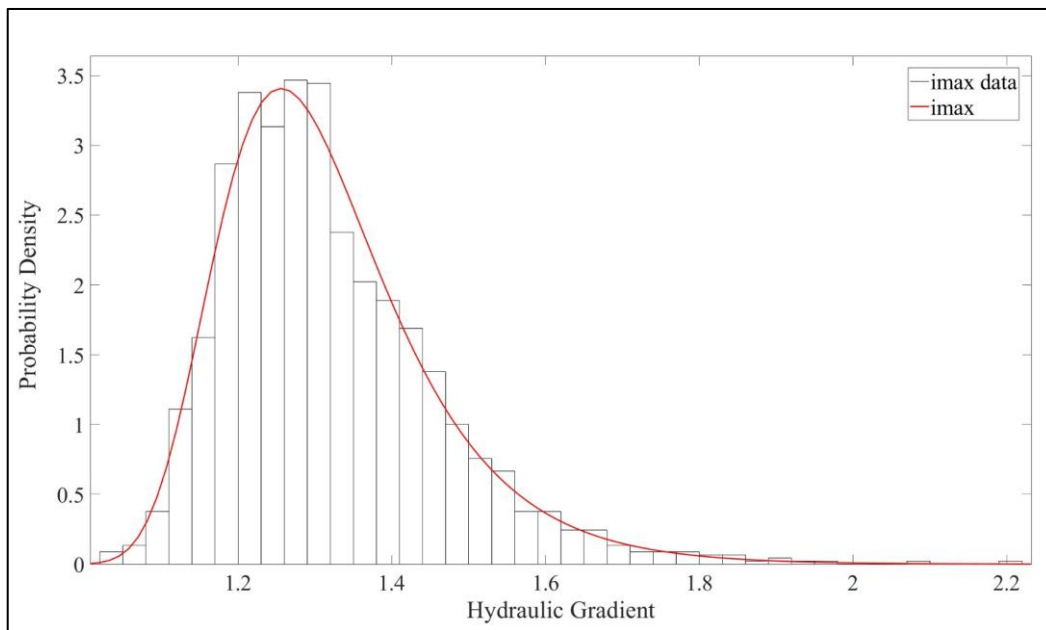
Figure 3.20 Generalized extreme value (GEV) distribution fit on i_{max} data

Then, the probability distributions of i_{max} and i_{crit} were plotted on the same figure and these are given in Figure 3.21 and Figure 3.22 for Terzaghi's i_{crit} and Tao's i_{crit}, respectively. Based on these figures, it appears that i_{max} values were consistently higher than i_{crit} values. Exceedance of the critical hydraulic gradient was important since it might result in increased seepage flows and initiation of motion of fine soil particles. This is further discussed in Chapter 4.

Figure 3.21 Probability distributions of Terzaghi's i_{crit} and i_{max}.
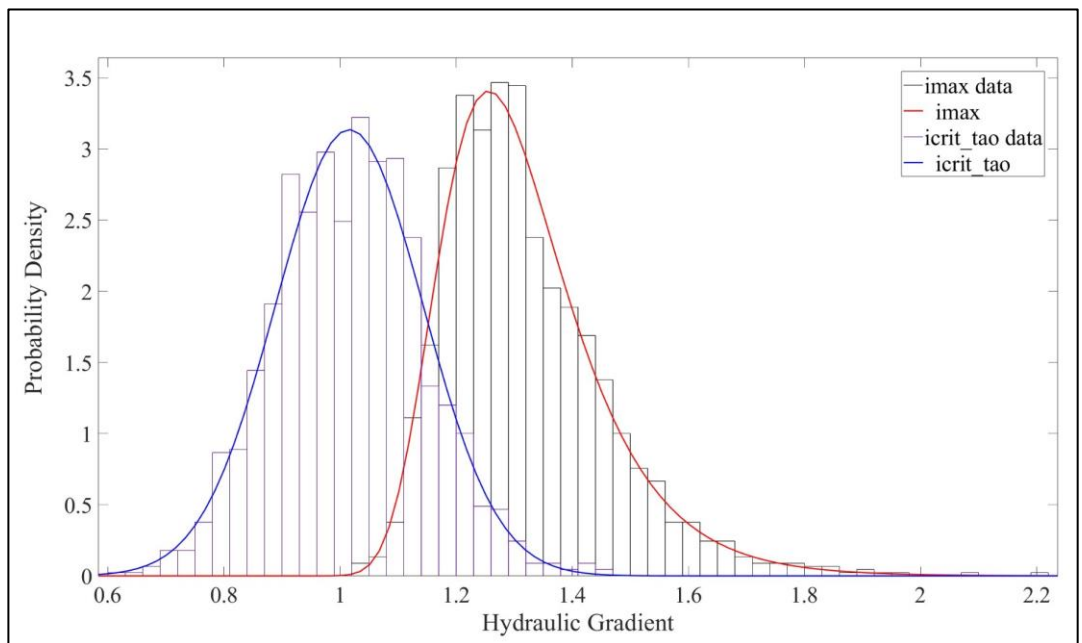
Figure 3.22 Probability distributions of Tao's i_{crit} and i_{max}.
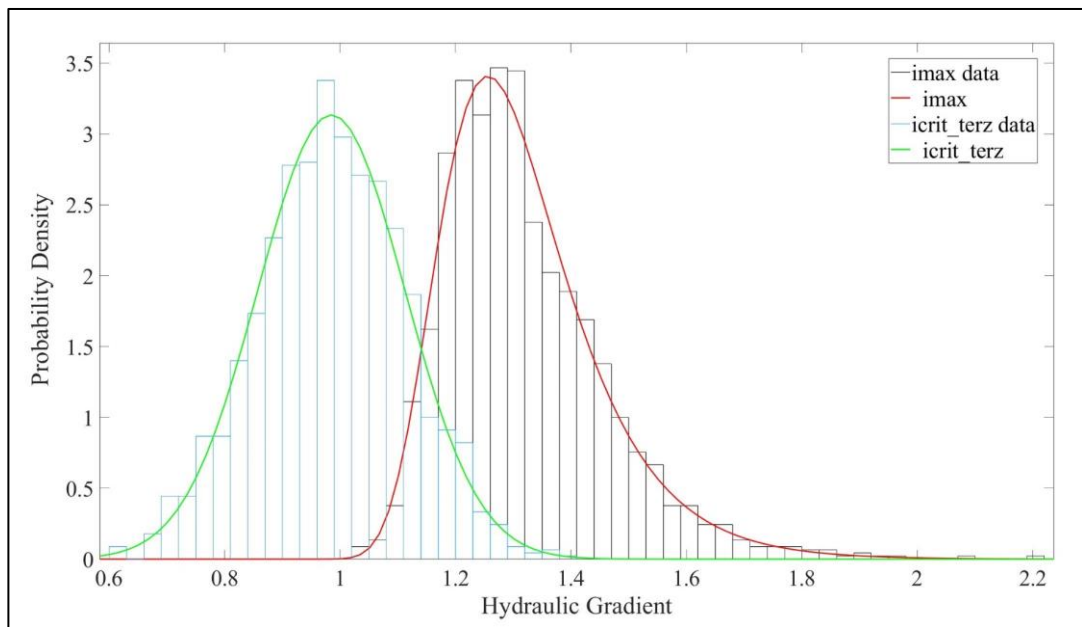
3.2.4 Exceedance Probability of the Critical Hydraulic Gradient

The i_{max} which followed GEV distribution was approximated using the Gumbel distribution, which is a Type-1 generalized extreme value distribution (Weisstein, 2023), for the sake of probability computations. The probability of exceedance of i_{crit} was computed with FORM and the results are given in Table 3.7. The results for the probability of exceedance of i_{crit} were obtained as 97% and 95% for Terzaghi's and Tao's models, respectively. Accordingly, there is an average of 96% probability that the critical hydraulic gradient is exceeded. The results are further discussed in detail in Chapter 4.

Table 3.7 Probability of exceedance of i_{crit}

Case	Probability of Exceedance
$i_{max} > i_{crit\_Terzaghi}$	0.97
$i_{max} > i_{crit\_Tao}$	0.95
Average	0.96

CHAPTER 4

DISCUSSION

4.1 General

The results given in Table 3.7 showed that there was around 96% probability of i_{max} exceeding i_{crit}, meaning, it is almost certain that the critical hydraulic gradient was exceeded. This can be interpreted as the soil particle motion was initiated; however, it was not an indication of internal erosion. For the internal erosion to take place, a certain pattern where developing hydraulic gradients are greater than the critical gradient is needed. To understand and discuss the likelihood of internal erosion in the application problem, further investigations were required. To this end, the results of the stochastic analyses were examined in more detail.

For this purpose, the locations of high values of hydraulic gradients were investigated on several randomly selected MCS runs. It was found that the maximum hydraulic gradient was consistently located near the toe of the dam in all simulations. This region is highlighted for some simulations in Figure 4.1-Figure 4.3 with a red circle. In the figures, high values of hydraulic gradients can be seen with yellow and orange colors. As can be seen from the figures, there were small localized zones with high hydraulic gradients and they were always surrounded by smaller and acceptable hydraulic gradient values that are smaller than the critical values. The gradients surrounding the localized high gradients zones were confirmed to be consistently less than 1. Considering that the mean value for the critical hydraulic gradient is around 1.0 for both Terzaghi's and Tao's models, in these regions, the soil particle motion had been initiated; however, particles that were in motion were immediately stopped and obstructed in the neighboring small gradient region, in other words, safe zones. Consequently, the calculated probability of exceedance of critical hydraulic gradient does not directly translate to the probability of internal erosion or piping.
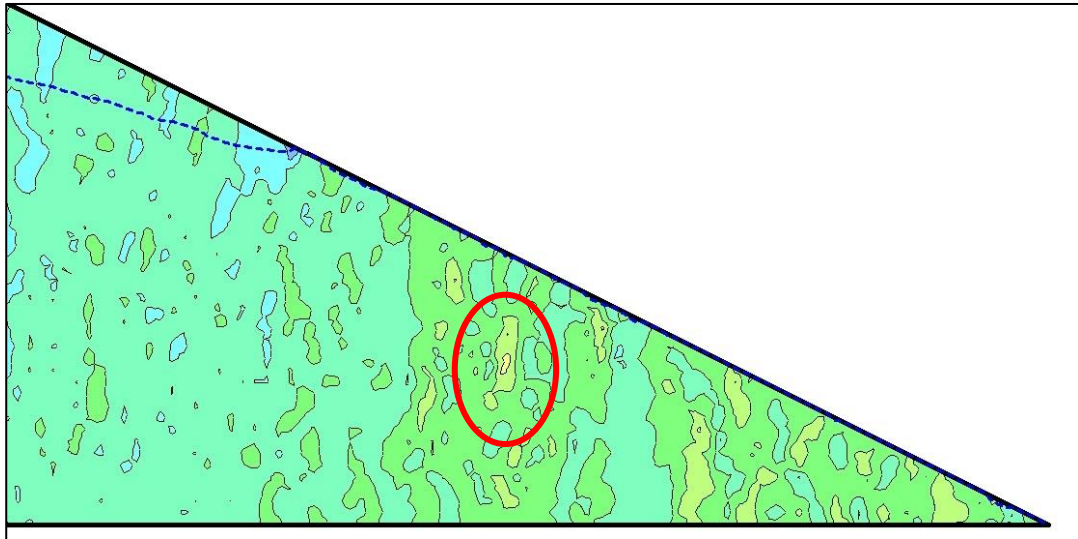
Figure 4.1 Example 1: x-gradient results from the toe of the dam for an example solution
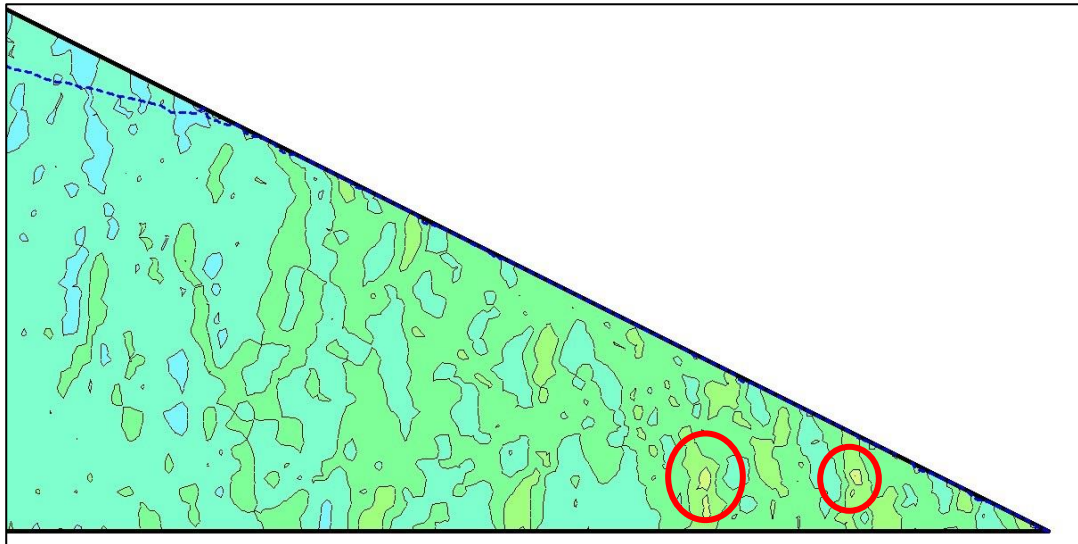

Figure 4.2 Example 2: x-gradient results from the toe of the dam for an example solution
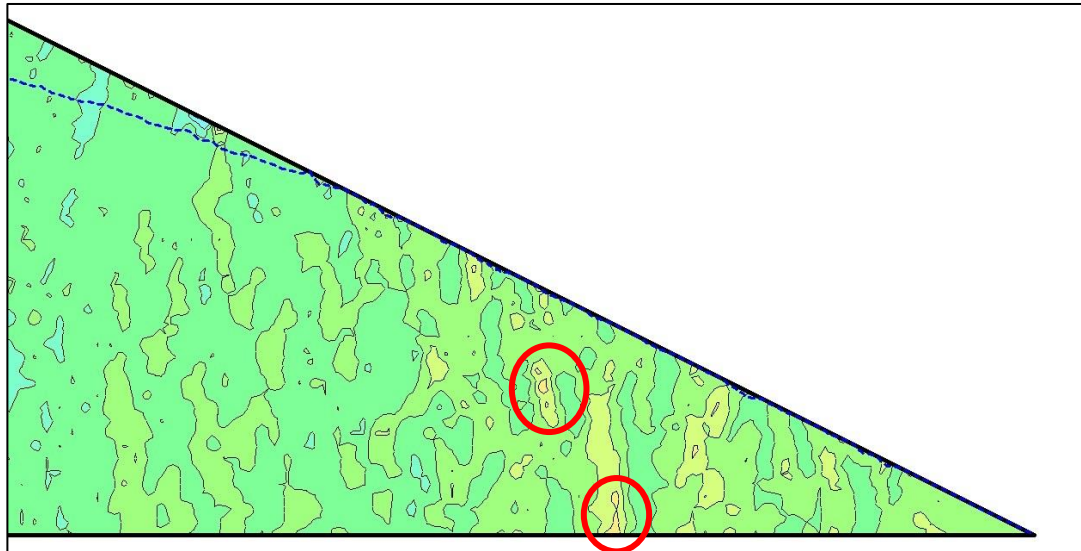
Figure 4.3 Example 3: *x*-gradient results from the toe of the dam for an example solution

Further studies were conducted to understand the reason behind the localized high-gradient regions that caused the exceedance probability to be considerably greater. In order to achieve this, a deterministic seepage analysis was conducted on the same earthen dam. This would show if the high hydraulic gradients were caused by the impact of the soil uncertainty, or the particular design of the dam. For ease of modeling, a saturated soil model was adopted, and the hydraulic conductivity was defined as a constant parameter with the average value given in Table 3.1 for the deterministic analysis. Figure 4.4 shows the contour lines of the *x*-gradients for the deterministic model. As can be seen from the figure, hydraulic gradients were reasonably small in the deterministic model. It was determined that the maximum gradient in the dam body was approximately 0.5 in the saturated zone, which was significantly less than the critical gradient. This was interpreted as the design of the dam was not the main cause of the soil particle motion in the stochastic models.

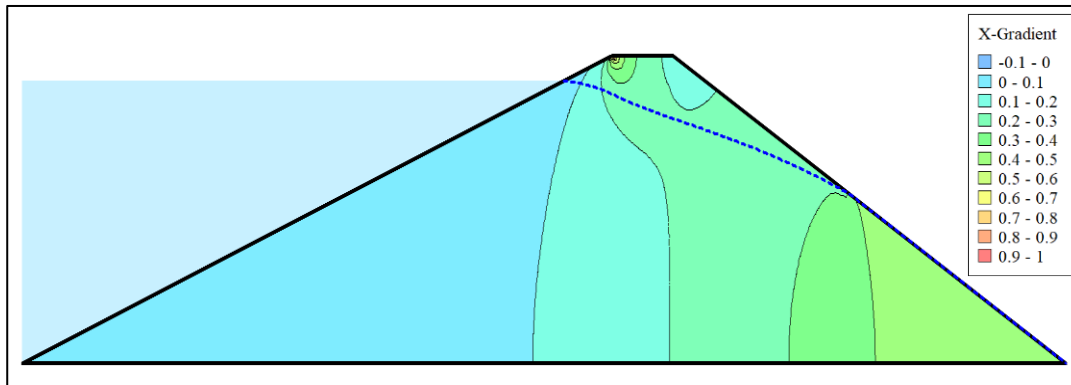Figure 4.4 The *x*-gradient contour lines for the deterministic model.

To explain the existence of high gradient zones and particle motion in stochastic models, it is necessary to understand the concept of hydraulic gradient. It represents the slope of the phreatic line of the seepage. If the slope is steep, the gradient is high. When Figure 3.12 is considered, the hydraulic conductivity of the stochastic model changes from one point to the other with a certain probability density function. This change may be abrupt since the hydraulic conductivity was not generated with a correlation function in the study; the parameters were generated without a dependence on each other even if they were located next to each other. This was one of the limitations of the stochastic numerical model. If two consecutive points have significantly different conductivity values, i.e., very high and low values, this would cause increased localized seepage with an abrupt change in the slope of the phreatic line and high hydraulic gradients. This was what happened for the stochastic models, and very high exceedance probabilities were observed.

4.2   Seepage Control Measures

Earthen dams are typically designed with measures to control and reduce seepage. However, the homogeneous earthen dam modeled in this study lacked such measures, making it vulnerable to seepage and internal erosion. Two example designs with seepage-controlling measures were investigated in the scope of the study to compare their seepage performance with that of the original dam. These

were modified homogeneous dams with a downstream toe drain and a blanket drain. Similar numerical models for these alternatives were established and deterministic seepage analyses were conducted. In both alternatives, the aim was to provide controlled drainage of the water in the dam body. The following design considerations were used in dimensioning both drains.

The drain lengths were selected based on the criteria suggested by Chahar (2004). It was suggested that the length of the drain should be selected according to the downstream slope cover which is shown with *d* in Figure 4.5.
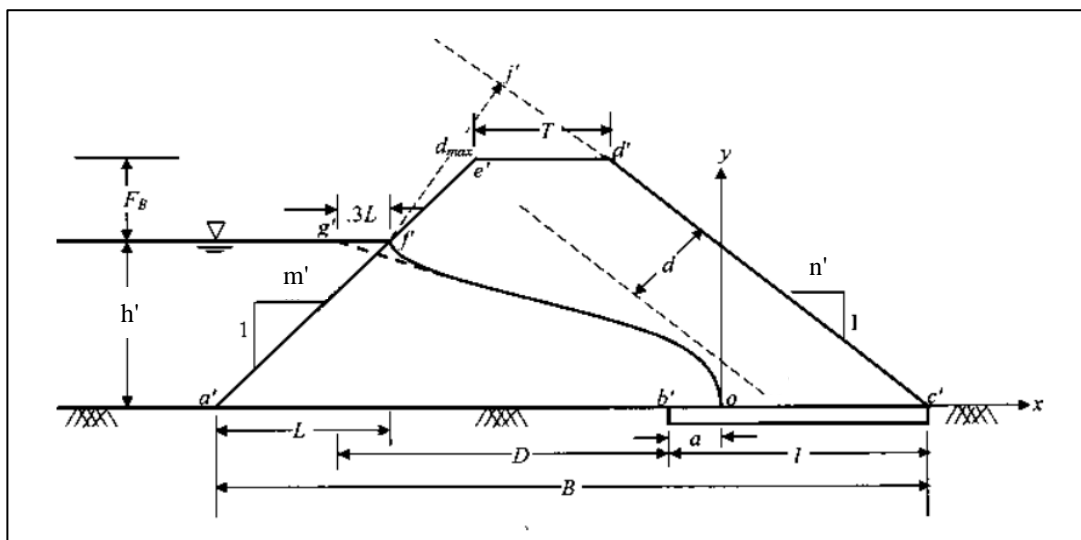
Figure 4.5 Drain length (*l*), downstream slope cover (*d*), and other dimensions used in the determination of drain length (Reprinted from Chahar, 2004)

The downstream slope cover, *d*, can be defined as the minimum distance of the phreatic line to the downstream face of the dam and therefore it is an important measure for safety against piping. Chahar (2004) proposed equations for the minimum drain length, l_{min}, (m) and maximum drain length, l_{max} (m) which are the lengths that provide no downstream slope cover and the maximum potential downstream slope cover, respectively. These equations are as follows:

$$l_{min} = \frac{1 + n'^2}{2n'} \Bigg(0.3m'h' + n'h' + F_B(m' + n') + T$$
$$- \sqrt{(0.3m'h' + n'h' + F_B(m' + n') + T)^2 - n'^2 h'^2} \Bigg)$$

(4.1)

$$l_{max}$$
$$= \frac{1 + n'^2}{2n'} \Bigg(0.3m'h' + n'h' + F_B(m' + n') + T + \frac{n'^2 - 1}{\sqrt{1 + n'^2}} d$$

(4.2)

$$- \sqrt{\left(0.3m'h' + n'h' + F_B(m' + n') + T - d\sqrt{1 + n'^2} \right)^2 - n'^2 h'^2} \Bigg)$$

where m' and n' are upstream and downstream face slopes of the dam, respectively, F_B (m) is the freeboard, T (m) is the crest width of the dam, h' (m) is the reservoir water depth and d (m) is the downstream slope cover. Using Eqs. (4.1) and (4.2), the minimum and maximum drain lengths were calculated as 8.5 m and 29.5 m, respectively. The drain length was selected as 25 m which provided a downstream slope cover of 6.4 m. The suggested height for the toe drain is about one-third of the reservoir depth (Singh & Varshney, 1995, Mishra & Parida, 2006) and the minimum thickness for the blanket drain is recommended as 1.0 m (USBR, 1987). Accordingly, a toe drain height of 8 m and a blanket thickness of 1.0 m were selected. Established numerical models are shown in Figure 4.6 and Figure 4.7 for the toe and blanket drain alternatives, respectively. The material shown with gray color in the figures is the main drain and was made of sandy gravel. It had a hydraulic conductivity of 0.004 m/s, which was much higher than that of the homogeneous fill material, clayey sand. The material shown with orange color is a filter layer that allows a gradual transition from the fine dam material to the coarser drain material. This layer is important for the stability of the dam since it prevents the dam material from getting washed away by seepage. The homogeneous fill material, clayey sand, had the average hydraulic conductivity presented in Table 3.1.
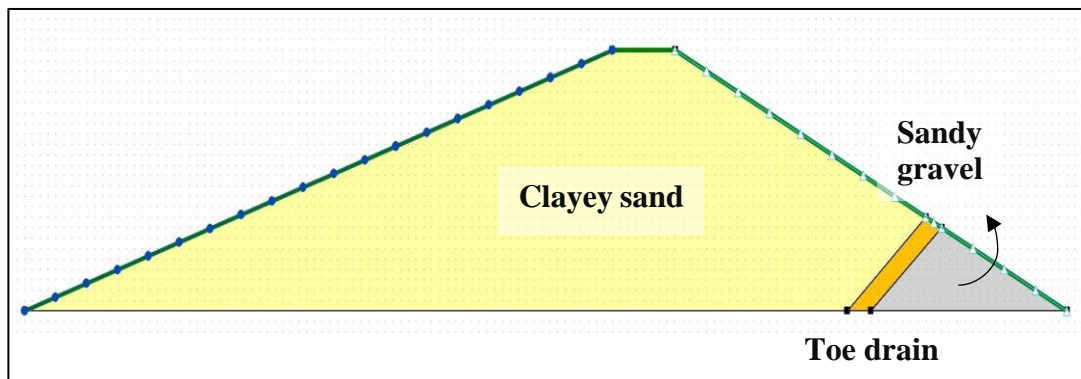
Figure 4.6 FEM model of the modified homogeneous earth dam with a toe drain.
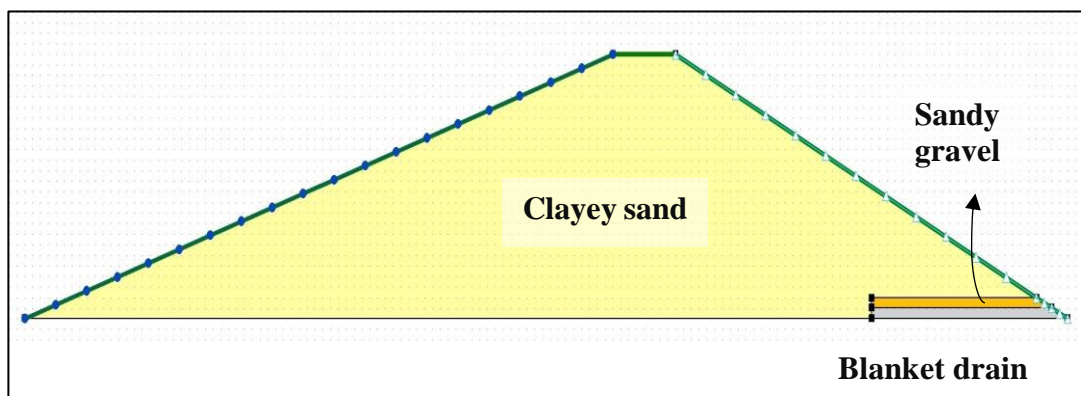
Figure 4.7 FEM model of the modified homogeneous earth dam with a blanket drain.

The seepage analyses for these alternatives were conducted using the saturated soil model with deterministic material properties for ease of computation. The analysis results showing the phreatic line and the x-gradient are given in Figure 4.8 and Figure 4.9. From the results, the downstream slope cover provided by the toe drain and blanket drain can be observed which is very critical for the safety of the earth dam against seepage-related problems. For these alternatives, even if there is a probability of particle movement initiation in the dam body, it is a lot less likely that this movement develops into internal erosion since seepage does not reach the downstream face of the dam and the dam material cannot get carried out.

The results revealed the downstream slope was better protected by the toe drain and blanket drain; no seepage face was developed with these alternatives. The phreatic

lines had a sharp slope at the region where the line met the drain and high hydraulic gradients were observed. However, the potential for particle movement initiation within the dam body does not necessarily lead to internal erosion. This is because the moving particles would be kept in the drain filter, significantly reducing the likelihood of them being carried away.
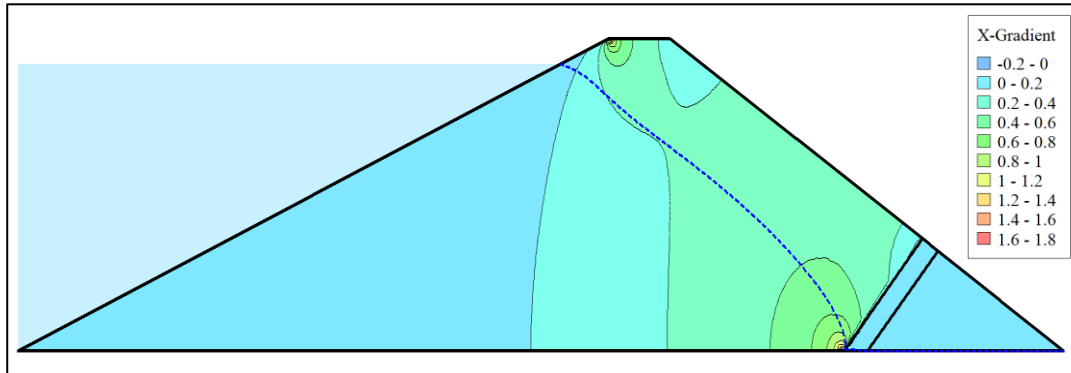

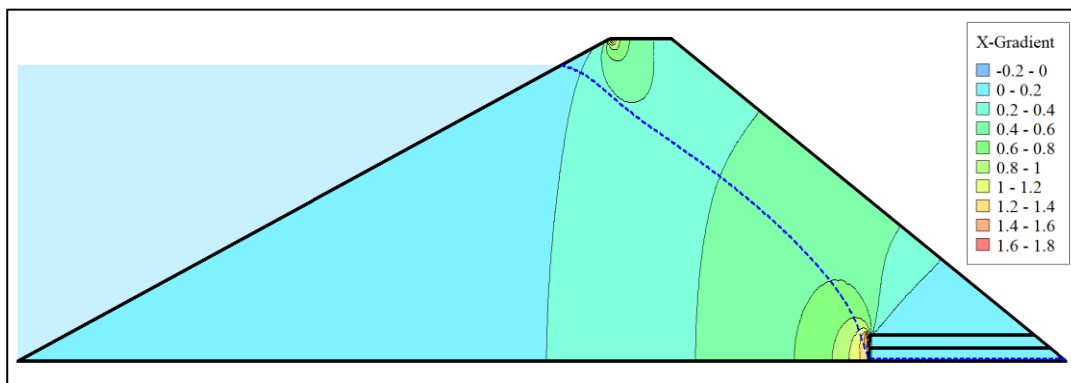Figure 4.8 *x*-gradient contour lines of the modified homogeneous earth dam with the toe drain

Figure 4.9 *x*-gradient contour lines for the modified homogeneous earth dam with the blanket drain

CHAPTER 5

CONCLUSION

5.1   Summary

Internal erosion leading to piping is the most common failure mode of earthen dams. Previous studies have developed critical head and hydraulic gradient models to assess safety against internal erosion. These critical values depend on soil properties in all these models. However, due to the uncertainties involved in soil properties, deterministic analysis may not be reliable for assessing internal erosion in earthen dams. This study presents a probabilistic model for seepage analysis of an earthen dam using the finite-element method and Monte Carlo simulations. The model considered the random nature of soil properties and their variability over the dam body. The hydraulic conductivity and soil water characteristic curve fitting parameters were defined as random variables with appropriate probability distributions. Monte Carlo simulations were used in combination with a random number generator to generate probability distributions of the maximum hydraulic gradient and the critical hydraulic gradient. The probability of exceedance of the critical hydraulic gradient was then computed to determine the probability of internal erosion for the earthen dam. The computed exceedance probabilities were found to be high and therefore the model results were investigated in more detail to interpret how this probability relates to the probability of internal erosion. In addition, two alternative earthen dam designs with seepage control measures were studied and their safety against internal erosion and piping were evaluated and compared with the original dam.

5.2 Findings of the Study

The main findings of the study can be summarized as follows:

- It was found that in earthen dams with completely random soil lacking a correlation structure, sharp phreatic surface slopes may occur, and high hydraulic gradients can be observed. This could result in critical hydraulic gradients being exceeded and soil particle motion initiation.

- Comparison of the critical and maximum hydraulic gradient distributions is a measure for the determination of the probability of soil particle motion. However, it is necessary to investigate further to determine if this could lead to internal erosion. To achieve this objective, the zones with high hydraulic gradients that exceed the critical values should be investigated. Then, the likelihood of internal erosion and piping can be interpreted.

- Particle movement initiation is likely to occur in certain areas of the dam body, which can result in internal erosion. Homogeneous dams lack measures to control seepage, and particle movement in these areas can lead to internal erosion and piping failure.

- The implementation of toe and blanket drains prevents the phreatic line from reaching the downstream face of the dam, leading to improved seepage control. These drains create a downstream slope cover for the earth dam, which can prevent particle movement and reduce the risk of internal erosion.

5.3 Suggested Future Work

The current study focused on the probability of exceedance of critical hydraulic gradient over the entire body of an earthen dam. However, there are more aspects that were not considered due to the research limitations, and these may be considered in future studies. These include but are not limited to consideration of the correlation structure of the random field, obtaining supportive data through experimental work, and inclusion of the dam foundation in the probabilistic model.

It was seen that not accounting for the soil correlation had some effects on the results. Taking it into account would give a better understanding of the probability of internal erosion. In addition, experimental studies can be conducted to understand the mechanism of internal erosion. A better understanding of the mechanism of particle movement developing into internal erosion could give a better idea of the relationship between the hydraulic gradients and internal erosion, as well as the areas prone to erosion. Furthermore, the probability of internal erosion in the foundations of all types of dams could be examined.

REFERENCES

Ang, A. H.-S., & Tang, W. H. (1975). *Probability Concepts in Engineering Planning and Design Vol. 1: Basic Principles: Vol. First*. John Wiley & Sons.

Ang, A. H.-S., & Tang, W. H. (1984). Probability concepts in engineering planning and design, vol. 2: Decision, risk, and reliability. In *JOHN WILEY & SONS, INC., 605 THIRD AVE., NEW YORK, NY 10158, USA, 1984, 608*.

ASDSO. (2023a, December 18). *Case Study: Baldwin Hills Dam (California, 1963)*. https://damfailures.org/case-study/baldwin-hills-dam/

ASDSO. (2023b, December 18). *Internal Erosion of Earth Dams*. https://damsafety.org/dam-owners/internal-erosion-of-earth-dams

Belcher, W., Camp, T., & Krzhizhanovskaya, V. V. (2016). Detecting erosion events in earth dam and levee passive seismic data with clustering. *Proceedings - 2015 IEEE 14th International Conference on Machine Learning and Applications, ICMLA 2015*, 903–910. https://doi.org/10.1109/ICMLA.2015.9

Bennion, D. W., & Griffiths, J. C. (1966). A Stochastic Model for Predicting Variations in Reservoir Rock Properties. *SPE Journal*, *6*(1), 9–16. https://doi.org/10.2118/1187-PA

Bligh, W. G. (1910). Dams, barrages and weirs on porous foundations. *Eng. News*, *64*(Dec), 708.

Bommes, D., Lévy, B., Pietroni, N., Puppo, E., Silva, C., Tarini, M., & Zorin, D. (2012). State of the art in quad meshing. *Eurographics-33rd Annual Conference of the European Association for Computer Graphics-2012*.

Box, G. E. P., & Muller, M. E. (1958). A Note on the Generation of Random Normal Deviates. *The Annals of Mathematical Statistics*, *29*(2), 610–611.

Brooks, R. H., & Corey, A. T. (1964). Properties of Porous Media Affecting Fluid Flow. *ASCE Journal of the Irrigation and Drainage Division*, *92*(2), 61–90.

Bulnes, A. C. (1946). An Application of Statistical Methods to Core Analysis Data of Dolomitic Limestone. *Transactions of the AIME*, *165*(1), 223–240. https://doi.org/10.2118/946223-G

Calamak, M. (2014). *Uncertainty Based Analysis of Seepage through Earth-fill Dams* [Ph.D. Thesis]. Middle East Technical University.

Calamak, M., Larocque, L. A., & Chaudhry, M. H. (2020). Numerical modelling of seepage through earthen dams with animal burrows: a case study. *Journal of Hydraulic Research*. https://doi.org/10.1080/00221686.2020.1780502

Calamak, M., Melih Yanmaz, A., & Kentel, E. (2017). Probabilistic evaluation of the effects of uncertainty in transient seepage parameters. *Journal of Geotechnical and Geoenvironmental Engineering*, *143*(9). https://doi.org/10.1061/(ASCE)GT.1943-5606.0001739

Calamak, M., & Yanmaz, A. M. (2017). Uncertainty quantification of transient unsaturated seepage through embankment dams. *International Journal of Geomechanics*, *17*(6). https://doi.org/10.1061/(ASCE)GM.1943-5622.0000823

Calamak, M., & Yanmaz, A. M. (2018). Assessment of core-filter configuration performance of rock-fill dams under uncertainties. *International Journal of Geomechanics*, *18*(4). https://doi.org/10.1061/(ASCE)GM.1943-5622.0001114

Carsel, R. F., & Parrish, R. S. (1988). Developing joint probability distributions of soil water retention characteristics. *Water Resources Research*, *24*(5), 755–769. https://doi.org/10.1029/WR024i005p00755

Chahar, B. R. (2004). Determination of length of a horizontal drain in homogeneous earth dams. *Journal of Irrigation and Drainage Engineering*, *130*(6), 530–536.

Fair, G. M., Hatch, L. P., & Hudson, H. E. (1933). Fundamental factors governing the streamline flow of water through sand [with discussion]. *Journal (American Water Works Association)*, *25*(11), 1551–1565.

FEMA. (2016). *Pocket Safety Guide for Dams and Impoundments*. https://www.fema.gov/sites/default/files/2020-08/fema_911_pocket_safety_guide_dams_impoundments_2016.pdf

Fernandes, M. M. (2020). *Analysis and design of geotechnical structures*. CRC Press.

Foster, M. (1999). *The probability of failure of embankment dams by internal erosion and piping* [Doctoral dissertation, The University of New South Wales Sydney, Australia]. https://doi.org/10.26190/unsworks/8289

Foster, M., Fell, R., & Spannagle, M. (2000). The statistics of embankment dam failures and accidents. *Canadian Geotechnical Journal*, *37*(5), 1000–1024. https://doi.org/10.1139/t00-030

Fredlund, D. G., & Xing, A. (1994). Equations for the soil-water characteristic curve. *Canadian Geotechnical Journal*, *31*(4), 521–532. https://doi.org/10.1139/t94-061

Fredlund, M. (2005). *SoilVision-A Knowledge Based Database System for Saturated/Unsaturated Soil Properties* (Version 4.21.001). SoilVision Systems Ltd.

GEOSLOPE International Ltd. (2022). *Heat and Mass Transfer Modeling*.

Kalateh, F., & Kheiry, M. (2023). A Review of Stochastic Analysis of the Seepage Through Earth Dams with a Focus on the Application of Monte Carlo Simulation. *Archives of Computational Methods in Engineering*, 1–26.

Khilar, K. C., Fogler, H. S., & Gray, D. H. (1985). Model for Piping-Plugging in Earthen Structures. *Journal of Geotechnical Engineering*, *111*(7), 833–846. https://doi.org/10.1061/(ASCE)0733-9410(1985)111:7(833)

Law, J. (1944). A Statistical Approach to the Interstitial Heterogeneity of Sand Reservoirs. *Transactions of the AIME*, *155*(1), 202–222. https://doi.org/10.2118/944202-G

Lu, N., & Likos, W. J. (2004). *Unsaturated Soil Mechanics*. John Wiley & Sons, Inc.

Marsaglia, G., & Tsang, W. W. (1984). A Fast, Easily Implemented Method for Sampling from Decreasing or Symmetric Unimodal Density Functions. *SIAM Journal on Scientific and Statistical Computing*, *5*(2), 349–359. https://doi.org/10.1137/0905026

Mesquita, M. da G. B. de F., Moraes, S. O., & Corrente, J. E. (2002). More adequate probability distributions to represent the saturated soil hydraulic conductivity. *Scientia Agricola*, *59*, 789–793.

Milligan, V. (2003). Some Uncertainties in Embankment Dam Engineering. *Journal of Geotechnical and Geoenvironmental Engineering*, *129*(9), 785–797. https://doi.org/10.1061/(ASCE)1090-0241(2003)129:9(785)

Mishra, G. C., & Parida, B. P. (2006). Earth dam with toe drain on an impervious base. *International Journal of Geomechanics*, *6*(6), 379–388.

Mooney, C. Z. (1997). *Monte Carlo simulation* (Issue 116). Sage.

Ojha, C. S. P., Singh, V. P., & Adrian, D. D. (2003). Determination of Critical Head in Soil Piping. *Journal of Hydraulic Engineering*, *129*(7), 511–518. https://doi.org/10.1061/(ASCE)0733-9429(2003)129:7(511)

Papagianakis, A. T., & Fredlund, D. G. (1984). A steady state model for flow in saturated–unsaturated soils. *Canadian Geotechnical Journal*, *21*(3), 419–430. https://doi.org/10.1139/t84-046

Pedarla, A., Puppala, A. J., Chittoori, B. S., Hoyos, L. R., Zapata, C., & Houston, S. L. (2012). *Influence of Mineral Montmorillonite on Soil Suction Modeling Parameters*.

Phoon, K., Santoso, A., & Quek, S. (2010). Probabilistic Analysis of Soil-Water Characteristic Curves. *Journal of Geotechnical and Geoenvironmental Engineering*, *136*(3), 445–455. https://doi.org/10.1061/(ASCE)GT.1943-5606.0000222

Redaelli, M. (2011). Estimating the probability of piping-induced breaching of flood embankments. In N. Vogt, B. Schuppener, D. Straub, & G. (Hg.) Bräu (Eds.), *Geotechnical Safety and Risk. ISGSR 2011* (pp. 567–576).

Richards, L. A. (1931). Capillary conduction of liquids through porous mediums. *Journal of Applied Physics*, *1*(5), 318–333.

Sako, K., & Kitamura, R. (2006). A Practical Numerical Model for Seepage Behavior of Unsaturated Soil. *SOILS AND FOUNDATIONS*, *46*(5), 595–604. https://doi.org/10.3208/sandf.46.595

Seed, H. B., & Duncan, J. M. (1987). The failure of Teton Dam. *Engineering Geology*, *24*(1), 173–205. https://doi.org/https://doi.org/10.1016/0013-7952(87)90060-3

Sellmeyer, J. B. (1988). *On the mechanism of piping under impervious structures* [Doctoral dissertation]. The Delft University of Technology .

Singh, B., & Varshney, R. S. (1995). Engineering for embankment dams. *(No Title)*.

Singh, V. P., Jain, S. K., & Tyagi, A. (2007). *Risk and Reliability Analysis: A Handbook for Civil and Environmental Engineers*. American Society of Civil Engineers Press.

Sivakumar Babu, G. L., & Srivastava, A. (2010). Reliability Analysis of Earth Dams. *Journal of Geotechnical and Geoenvironmental Engineering*, *136*(7), 995–998. https://doi.org/10.1061/(ASCE)GT.1943-5606.0000313

Tao, H. (2018). *Numerical modeling of soil internal erosion mechanism* [Doctoral dissertation]. University of Akron.

Terzaghi, K. (1929). Effect of minor geologic details on the safety of dams. *Amer. Inst. Min. and Met. Engrs. Tech. Publ.*, *215*, 31–44.

USBR. (1987). *Design of Small Dams*. United States Bureau of Reclamation.

van Genuchten, M. T. (1980). A Closed-form Equation for Predicting the Hydraulic Conductivity of Unsaturated Soils1. *Soil Science Society of America Journal*, *44*(5), 892–898. https://www.soils.org/publications/sssaj/abstracts/44/5/892

Vu, T., Loehr, E., & Smith, D. (2018). Probabilistic analysis and resistance factor calibration for deep foundation design using Monte Carlo simulation. *Heliyon*, *4*(8), e00727. https://doi.org/https://doi.org/10.1016/j.heliyon.2018.e00727

Warren, J. E., & Price, H. S. (1961). Flow in Heterogeneous Porous Media. *SPE Journal*, *1*(3), 153–169. https://doi.org/10.2118/1579-G

Warrick, A. W., & Nielsen, D. R. (1980). 13 - Spatial Variability of Soil Physical Properties in the Field. In D. HILLEL (Ed.), *Applications of Soil Physics* (pp. 319–344). Academic Press. https://doi.org/https://doi.org/10.1016/B978-0-12-348580-9.50018-3

Weisstein, E. W. (2023, December 23). *Extreme Value Distribution*. https://mathworld.wolfram.com/ExtremeValueDistribution.html

Willardson, L. S., & Hurst, R. L. (1965). Sample Size Estimates in Permeability Studies. *Journal of the Irrigation and Drainage Division*, *91*(1), 1–10.

Xie, Q., Liu, J., Han, B., Li, H., Li, Y., & Li, X. (2018). Critical hydraulic gradient of internal erosion at the soil–structure interface. *Processes*, *6*(7), 92.

Yücemen, S. (2021). *Risk and Reliability Models [Lecture Notes]. Middle East Technical University, Ankara/Turkey, CE589*.

APPENDICES

A. MATLAB codes used in MCS for generating i_{crit} datasets

MATLAB code for generating i_{crit} dataset based on Terzaghi's Model:

```
clear;
close all;
clc;

% Creates the probability distribution of critical hydraulic gradient for
an earthen embankment using
% Terzaghi's model. Buoyant unit weight of the dam material(GamaS) is
represented
% with a normal distribution

% Input
GamaW = 9.81;           % (kN/m3) unit weight of water
m_GamaS = 9.63;         % mean buoyant unit weight of the dam material
sigma_GamaS =  1.26;    % standard deviation of buoyant unit weight of
the dam material
sample = 1500;          % number of sample size to be created

% Calculation Stage
icrit = zeros(sample,1);
GamaS = zeros(sample,1);
for i = 1:sample
GamaS(i) = normrnd(m_GamaS,sigma_GamaS);
icrit(i) = GamaS(i)/GamaW;      % critical hydraulic gradient
end
```

MATLAB code for generating i_{crit} dataset based on Tao's Model:

```
clear;
close all;
clc;

% Creates the probability distribution of critical hydraulic gradient for
an earthen embankment using
% Tao(2018)'s model. Specific gravity (Gs) is represented with normal and
void ratio (e) is represented with  lognormal distribution

% Input
mu_Gs = 2.687              % Mean specific gravity of soil (normal)
sigma_Gs = 0.126           % St. dev. of the specific gravity of soil
(normal)
mu_e = -0.333              % Mean void ratio (lognormal)
sigma_e = 0.247            % St. dev. of the void ratio (lognormal)
SF = 6.1                   % Shape Factor defined in Tao(2018)
sample = 1500              % number of sample size to be created

% Calculation Stage
icrit = zeros(sample,1);
Gs = zeros(sample,1);
e = zeros(sample,1);
for i = 1:sample
Gs(i) = normrnd(mu_Gs,sigma_Gs);
e(i) = lognrnd(mu_e,sigma_e);
icrit(i) = (Gs(i)-1)*(SF/6)^2/(1+e(i));     % critical hydraulic gradient
end
```